A Two-Step Certified Reduced Basis Method*

J.L. Eftang† D.B.P. Huynh‡ D.J. Knezevic‡
A.T. Patera‡

Abstract

In this paper we introduce a two-step Certified Reduced Basis (RB) method. In the first step we construct from an expensive finite element "truth" discretization of dimension $\mathcal{N}$ an intermediate RB model of dimension $N \ll \mathcal{N}$. In the second step we construct from this intermediate RB model a *derived* RB (DRB) model of dimension $M \leq N$. The construction of the DRB model is effected at cost $\mathcal{O}(N)$ and in particular at cost independent of $\mathcal{N}$; subsequent evaluation of the DRB model may then be effected at cost $\mathcal{O}(M)$. The DRB model comprises both the DRB output *and* a rigorous *a posteriori* error bound for the error in the DRB output with respect to the *truth* discretization.

The new approach is of particular interest in two contexts: *focus calculations* and *hp-RB approximations*. In the former the new approach serves to reduce online cost, $M \ll N$: the DRB model is restricted to a slice or subregion of a larger parameter domain associated with the intermediate RB model. In the latter the new approach enlarges the class of problems amenable to *hp*-RB treatment by a significant reduction in offline (precomputation) cost: in the development of the *hp* parameter domain partition and associated "local" (now derived) RB models the finite element truth is replaced by the intermediate RB model. We present numerical results to illustrate the new approach.

Keywords: two-step model reduction; derived reduced basis; focus calculations; *hp* reduced basis.

1 Introduction

The Certified Reduced Basis (RB) method is a computational and mathematical framework for model order reduction of parameter dependent partial differential equations (PDEs). In particular, the RB method provides rapid and certifiable

*May 6, 2011. Springer Journal of Scientific Computing, DOI: 10.1007/s10915-011-9494-2

†Department of Mathematical Sciences, Norwegian University of Science and Technology, Trondheim, Norway, eftang@math.ntnu.no.

‡Department of Mechanical Engineering, Massachusetts Institute of Technology, Cambridge, MA, USA, {huynh, dknez, patera}@mit.edu.

computation of linear functional outputs — such as average field values or average fluxes — associated with the solution to the PDE for any set of input parameter values that configure the PDE in terms of (say) applied forces, material properties, geometry, or boundary conditions. The RB method is of interest in two particular contexts: *real-time* — such as parameter estimation [23] and optimal control [13] — and *many-query* — such as multiscale [3, 20] or stochastic simulation [4]. In these contexts, a computational preprocessing (offline) stage is typically justified. Early contributions to the RB methodology include [1, 24, 25]. For a review of these as well as more recent contributions, we refer to [26].

Given any input parameter value from a predefined parameter domain, the RB field approximation is a Galerkin-optimal linear combination of N precomputed highly accurate ("truth") $\mathcal{N}$-degree-of-freedom Finite Element (FE) snapshots of the solution to the PDE associated with N judiciously chosen parameter values. The RB output approximation is then evaluated as a linear functional of the RB field approximation. When the solution depends smoothly on the parameters an accurate RB approximation may be computed based on rather few precomputed snapshots: $N \ll \mathcal{N}$. Moreover, a rigorous *a posteriori* RB output error bound for the difference between the truth output and RB output may also be developed.

The efficiency of the RB method in the real-time and many-query contexts is effected through an *offline-online* computational strategy. The RB *offline* stage comprises FE snapshot selection and computation. This stage may be expensive — $\mathcal{N}$-dependent — but is performed only once as preprocessing. The RB *online* stage comprises evaluation of the RB output *and* RB output error bound for any given input parameter value. This stage is inexpensive — $\mathcal{N}$-independent — and may thus be effected in real-time and many-query contexts. The keys to the $\mathcal{N}$-independent online stage are efficient *construction–evaluation* computational procedures that link the offline and online stages through a stored dataset of size independent of $\mathcal{N}$. These procedures also provide efficient and exhaustive exploration of the parameter domain in the offline selection of optimal FE snapshots through a Greedy sampling algorithm.

In this paper we introduce a two-step Certified RB method. In the first step we construct from an expensive FE truth discretization of dimension $\mathcal{N}$ an intermediate RB model of dimension $N \ll \mathcal{N}$. In the second step we construct from this intermediate RB model a *derived* RB (DRB) model of dimension $M \leq N$. The construction of the DRB model is effected at cost $\mathcal{O}(N)$ and in particular at cost independent of $\mathcal{N}$; subsequent evaluation of the DRB model may then be effected at cost $\mathcal{O}(M)$. The DRB model comprises both the DRB output *and* a rigorous *a posteriori* error bound for the error in the DRB output with respect to the *truth* discretization.

The DRB model is defined over a parameter *subdomain* (typically a subregion or submanifold of the original parameter domain associated with the underlying intermediate RB model) and hence typically M can be chosen significantly smaller than N; the DRB model thus enables an additional speedup. The key innovations of this paper are efficient DRB precomputation — the *con-*

struction cost of the DRB model is $\mathcal{N}$-independent — and rigorous and efficient *a posteriori* bounds for the error in the DRB approximation — the error may be bounded rigorously with respect to the $\mathcal{N}$-complexity FE truth at *evaluation cost* independent of $\mathcal{N}$ *and* N.

The notion of two-step model order reduction has been considered in earlier works, albeit in different contexts and with different emphasis than our approach here. In [29], a "Fourier model reduction method" for large (non-parametric) control problems is presented. The Fourier method is first applied to the original equation in order to construct an "intermediate order" reduced system; a computationally more intensive reduction method, such as balanced truncation [22], may then be applied to this intermediate order system. A two-step strategy is also pursued in [18], where a Krylov subspace method is followed by balanced truncation in the context of circuit component design.

In this paper, we consider parametric model order reduction in two contexts in which our new approach is of particular interest:

Focus calculations. We consider the case in which we require many (or real-time) RB output evaluations in a parameter subdomain or submanifold $\mathcal{D}' \subset \mathcal{D}$. For an accurate approximation over this smaller parameter subdomain, a smaller DRB model may be sufficient and hence provide faster output computation compared to the standard RB alternative. Applications include parameter estimation and in particular Bayesian inference [23] and frequentistic validation [14], as well as visualization or indeed design or optimization of an RB output or RB error bound over a 1-parameter or 2-parameter slice of the full parameter domain.

***hp*-RB approximation.** The *hp*-RB method was recently introduced in [7]. This approach provides an online speedup of the RB approximation through an optimal and automatic partition (*h*-refinement) of the full parameter domain $\mathcal{D}$ into K parameter subdomains $\mathcal{V}^k \subset \mathcal{D}$, $1 \le k \le K$. A standard RB model of dimension N^k is then constructed for each parameter subdomain (*p*-refinement); presumably we may choose $N^k \ll N$ since each "local" approximation space is invoked for a smaller range of parameter values. However, although the online speedup associated with an *hp*-RB approximation may be significant, the offline cost can be rather large: the dimension reduction effected within each subdomain does not balance the number of parameter subdomains in terms of total offline computational cost. Thus, in particular, the *hp*-RB offline stage requires $N_{\text{total}} = \sum_{k=1}^{K} N^k > N$ truth FE snapshot computations in total.

With the new two-step approach introduced in this paper, we replace the N_{total} expensive offline FE truth snapshot computations in the *hp*-RB offline stage with much less expensive RB snapshot approximations; we then replace the standard RB model associated with each parameter subdomain by a DRB model. Through this *hp*-DRB approach, we may significantly reduce the *hp*-RB offline cost and hence broaden the class of problems amenable to *hp*-RB treatment. We include a summary of the *hp*-RB method in Section 5.1.

We may also pursue a mixed approach (for focus calculations or *hp*-RB approximations), in which the underlying intermediate RB model is in fact an *hp*-RB model. However, in particular with an *hp*-DRB approach, there is in this case a delicate balance in the offline stage between additional FE snapshot computations (for the underlying *hp*-RB model) and faster *hp*-RB snapshot computation (for the DRB models). We do not consider this mixed approach further in this paper.

The paper is organized as follows. We introduce in Section 2 the problem statement as well as notation required later; we also introduce two model problems to which we shall apply the new method. We introduce in Section 3 the new two-step approximation scheme; we discuss the (Greedy) construction of the RB and DRB approximation spaces, *a posteriori* error estimation, and the associated (construction-evaluation) computational procedures. We consider in Section 4 and Section 5 the new approach in the context of focus calculations and in the context of *hp*-RB approximations, respectively. In each context we discuss the associated offline-online computational decoupling, and we present numerical results for our two model problems; for all our numerical results we use `rbOOmit` [21], which is an RB plugin for the open source FE library `libMesh` [19]. Finally, in Section 6, we summarize the paper and discuss some areas of future work.

2 Problem Statement

2.1 Abstract Framework

We consider linear elliptic second order partial differential equations. For simplicity in the exposition of our approach we consider the formulation only for real-valued fields, however the extension to complex fields is straightforward and in fact in our second model problem (Helmholtz acoustic horn) we present results for this complex case. We introduce the spatial domain $\Omega \subset \mathbb{R}^d$ $(d = 1, 2, 3)$; we shall denote a particular spatial point $x \in \Omega$ as $x = (x_{(1)}, \ldots, x_{(d)})$. We further specify the function spaces $L_2(\Omega) = \{v : \int_\Omega v^2 < \infty\}$, $H_1(\Omega) = \{|\nabla v| \in L^2(\Omega)\}$, and $H_0^1(\Omega) = \{v \in H^1(\Omega), v|_{\partial\Omega} = 0\}$; we then introduce the space X^e associated with the exact solutions of the parametrized PDE as $H_0^1(\Omega) \subseteq X^e \subseteq H^1(\Omega)$. We next introduce a parameter domain $\mathcal{D} \subset \mathbb{R}^P$; we shall denote a particular parameter value $\mu \in \mathcal{D}$ as $\mu = (\mu_{(1)}, \ldots, \mu_{(P)})$.

We next introduce a parametrized bilinear form a and a parametrized linear functional f such that for any parameter value $\mu \in \mathcal{D}$, $a(\cdot, \cdot; \mu) : X^e \times X^e \to \mathbb{R}$ is coercive and continuous over X^e, and $f(\cdot; \mu) : X^e \to \mathbb{R}$ is bounded over X^e. We also introduce an X^e-bounded linear output functional $\ell : X^e \to \mathbb{R}$ which we for simplicity assume is parameter independent. We shall further assume

that a and f admit parametrically affine expansions

$$a(\cdot,\cdot;\mu) = \sum_{q=1}^{Q_a} a^q(\cdot,\cdot)\Theta_a^q(\mu), \tag{2.1}$$

$$f(\cdot;\mu) = \sum_{q=1}^{Q_f} f^q(\cdot)\Theta_f^q(\mu), \tag{2.2}$$

respectively, where $Q_a \leq Q$, $Q_f \leq Q$, and Q is finite and relatively small. The assumptions (2.1) and (2.2) accommodate the construction-evaluation computational procedures which we shall discuss in detail in Section 3.4. However, we note that these assumptions may be relaxed by the Empirical Interpolation Method [2, 5, 10], which in the non-affine case serves to construct affine expansions that are good approximations to the non-affine forms.

We denote by $\bar{\mu} \in \mathcal{D}$ a fixed "reference" parameter value; we then introduce the X-inner product and the associated X-norm for any $v, w \in X^e$ as

$$(w,v)_X = \frac{1}{2}(a(w,v;\bar{\mu}) + a(v,w;\bar{\mu})), \qquad \|v\|_X = \sqrt{(v,v)_X}, \tag{2.3}$$

respectively (more generally we may consider any inner product with induced norm equivalent to $\|\cdot\|_X$). We further introduce the coercivity and continuity constants of a,

$$\alpha^e(\mu) = \inf_{v\in X^e} \frac{a(v,v;\mu)}{\|v\|_X^2}, \quad \gamma^e(\mu) = \sup_{v\in X^e}\sup_{w\in X^e} \frac{a(v,w;\mu)}{\|v\|_X\|w\|_X}, \tag{2.4}$$

respectively.

We may now introduce the abstract formulation of the exact problem. Given any parameter value $\mu \in \mathcal{D}$, find $u^e(\mu) \in X^e$ such that

$$a(u^e(\mu), v;\mu) = f(v;\mu), \quad \forall v \in X^e, \tag{2.5}$$

and then evaluate the exact output of interest as

$$s^e(\mu) = \ell(u^e(\mu)). \tag{2.6}$$

We next introduce a high-fidelity truth FE approximation space $X \equiv X^{\mathcal{N}} \subset X^e$ of finite dimension $\mathcal{N}$. We may then introduce the truth FE discretization of (2.5)–(2.6): given any $\mu \in \mathcal{D}$, find $u(\mu) \in X$ such that

$$a(u(\mu), v;\mu) = f(v;\mu), \quad \forall v \in X, \tag{2.7}$$

and then evaluate the truth output of interest as

$$s(\mu) = \ell(u(\mu)). \tag{2.8}$$

We shall assume that X is chosen rich enough (and thus $\mathcal{N}$ large enough) that, for any $\mu \in \mathcal{D}$, the error between the exact solution $u^e(\mu)$ and the truth

approximation $u(\mu)$ is negligible at the desired level of numerical accuracy for the RB approximation; the RB approximation shall be built upon, and the RB error shall be bounded with respect to, this FE truth approximation.

We now introduce the coercivity and continuity constants of a with respect to X,

$$\alpha(\mu) = \inf_{v \in X} \frac{a(v, v; \mu)}{\|v\|_X^2}, \quad \gamma(\mu) = \sup_{v \in X} \sup_{w \in X} \frac{a(v, w; \mu)}{\|v\|_X \|w\|_X}, \tag{2.9}$$

respectively; for our *a posteriori* error estimators, we shall also require a coercivity lower bound $\alpha_{\rm LB}$: $0 < \alpha_{\rm LB}(\mu) \leq \alpha(\mu)$, for all $\mu \in \mathcal{D}$. An efficient computational procedure for the computation of a coercivity lower bound is possible through the Successive Constraint Method (SCM) [16, 17, 26].

The RB method [26] provides an acceleration of the truth (2.7)–(2.8) by the construction of an approximation space of low dimension $N \ll \mathcal{N}$. This space is optimized for the particular problem at hand, and thus provides accurate approximations despite the relatively low cost. The DRB method, which is the focus of this paper, further accelerates the RB approximation in contexts such as focus calculations and *hp*-RB approximations by the construction of an approximation space *derived* from an intermediate RB approximation space. This DRB approximation space is tailored to a parameter subdomain or submanifold of the original parameter domain, and is of even lower dimension $M \leq N$.

2.2 Model Problems

2.2.1 A 3D Thermal Block

We introduce here a "thermal block" linear elliptic model problem. We specify the spatial domain (the thermal block) $\Omega = (0, 1)^3$, which is partitioned into eight subblocks

$$\Omega_0 = (0, 0.5) \times (0, 0.5) \times (0, 0.5), \tag{2.10}$$
$$\Omega_1 = (0.5, 1) \times (0, 0.5) \times (0, 0.5), \tag{2.11}$$
$$\Omega_2 = (0, 0.5) \times (0.5, 1) \times (0, 0.5), \tag{2.12}$$
$$\Omega_3 = (0.5, 1) \times (0.5, 1) \times (0, 0.5), \tag{2.13}$$
$$\Omega_4 = (0, 0.5) \times (0, 0.5) \times (0.5, 1), \tag{2.14}$$
$$\Omega_5 = (0.5, 1) \times (0, 0.5) \times (0.5, 1), \tag{2.15}$$
$$\Omega_6 = (0, 0.5) \times (0.5, 1) \times (0.5, 1), \tag{2.16}$$
$$\Omega_7 = (0.5, 1) \times (0.5, 1) \times (0.5, 1), \tag{2.17}$$

as shown in Figure 2.1. We shall consider the nondimensionalized temperature $u^e(\mu)$ in Ω. We specify unity (inward) heat flux on the floor $\Gamma_{\rm base} = \{x \in \partial\Omega : x_{(3)} = 0\}$; we specify thermal insulation $\partial u^e / \partial n = 0$ on the walls $\Gamma_{\rm wall} = \{x \in \partial\Omega : x_{(1)} = 0 \text{ or } x_{(1)} = 1\} \cup \{x \in \partial\Omega : x_{(2)} = 0 \text{ or } x_{(2)} = 1\}$ (here n denotes the outward normal unit vector); and we specify zero temperature $u^e = 0$ on the top $\Gamma_{\rm top} = \{x \in \partial\Omega : x_{(3)} = 1\}$. We require continuity of the temperature and of

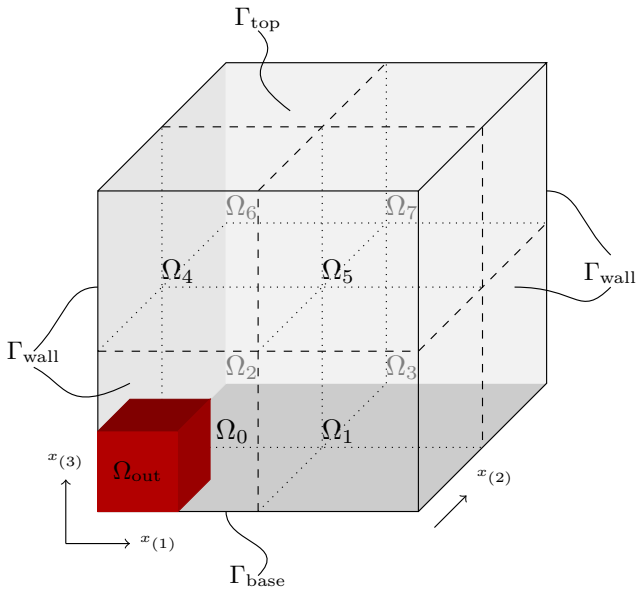

Figure 2.1: The thermal block.

the heat flux across interior boundaries. We next specify the parameter domain $\mathcal{D} = [0.5, 2]^7$; the thermal conductivity in the seven subblocks Ω_i, $1 \le i \le 7$, is given by $\mu_{(i)}$, $1 \le i \le 7$. The thermal conductivity in Ω_0 is equal to unity.

We now specify the exact space $X^e = \{v \in H^1(\Omega) : v|_{\Gamma_{\text{top}}} = 0\}$. We then specify, for all $\mu \in \mathcal{D}$ and for any $w, v \in X^e$, the bilinear form and linear functional

$$a(w, v; \mu) = \int_{\Omega_0} \nabla w \cdot \nabla v + \sum_{i=1}^{7} \mu_{(i)} \int_{\Omega_i} \nabla w \cdot \nabla v, \tag{2.18}$$

$$f(v; \mu) = \int_{\Gamma_{\text{base}}} v, \tag{2.19}$$

respectively. We also specify, for any $v \in X^e$, the output functional

$$\ell(v) = \frac{1}{|\Omega_{\text{out}}|} \int_{\Omega_{\text{out}}} v, \tag{2.20}$$

where $\Omega_{\text{out}} = (0, 0.25) \times (0, 0.25) \times (0, 0.25)$ and $|\Omega_{\text{out}}| = 0.25^3$ is the size of Ω_{out}. The exact weak formulation for the temperature $u^e(\mu)$ in Ω is then given by (2.5); the exact output $s^e(\mu) = \ell(u^e(\mu))$ corresponds to the average temperature over Ω_{out}. We note that our affine assumptions (2.1)–(2.2) hold for $Q_a = 8$ and $Q_f = 1$. We choose for this problem the reference parameter $\bar{\mu} = (1, 1, 1, 1, 1, 1, 1) \in \mathbb{R}^7$; thus $(w, v)_X = \int_\Omega \nabla w \cdot \nabla v$.

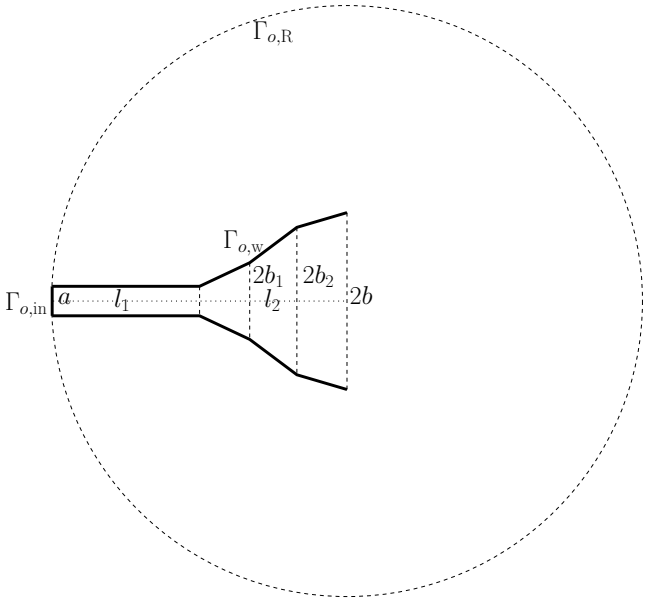

Figure 2.2: The acoustic horn.

For our numerical results of Section 4.2.1 (focus calculations) and Section 5.4.1 (*hp*-RB approximations) we use for our truth calculations a standard $\mathbb{P}_1(\Omega)$ FE approximation space $X = X^{\mathcal{N}}$ of dimension $\mathcal{N} = 9261$, which is deemed sufficiently rich. The truth FE formulation of the problem is then given by (2.7). We note that with our choice of inner product our problem is coercive with a coercivity lower bound given for all $\mu \in \mathcal{D}$ by $\alpha_{\mathrm{LB}}(\mu) = \min\{1, \mu_{(1)}, \cdots, \mu_{(7)}\}$. (In fact here $\alpha_{\mathrm{LB}}(\mu) \leq \alpha^e(\mu)$ $(\leq \alpha(\mu))$.)

2.2.2 A 2D Acoustic Horn

We introduce here a Helmholtz linear elliptic model problem, first proposed in [27]. We specify a parametrized two-dimensional domain $\Omega_o(\mu) \subset \mathbb{R}^2$, which corresponds to a parameter dependent acoustic horn inside a truncated circular domain as shown in Figure 2.2. (The subscript $_o$ denotes an "original" quantity; for our computational procedures we consider $\Omega_o(\mu)$ as the image of a parameter independent "reference" domain under a piecewise affine mapping.) The horn consists of a straight channel of width $a = 1$ and length $l_1 = 3$, followed by a flared section of length $l_2 = 5$. The outlet is of width $2b = 10$. The expansion channel is divided into 3 sections of equal length 5/3. The wall $\Gamma_{o,\mathrm{W}}$ of the symmetric expansion channel is modeled as a piecewise linear function; the heights of the sections, b_1 and b_2, are considered as our (geometric) parameters. The domain is truncated at the circle $\Gamma_{o,\mathrm{R}}$ of radius $R = 12.5$ centered slightly away from the outlet of the horn.

We shall consider the nondimensionalized (complex) pressure $u_o^e(\mu)$ in $\Omega_o(\mu)$; in this subsection $i = \sqrt{-1}$. We specify a source, $\dfrac{\partial u_o^e(\mu)}{\partial n_o} + i\mu_{(3)} u_o^e(\mu) = 2i\mu_{(3)}$, at the inlet $\Gamma_{o,\text{in}}$; we specify a first order (Sommerfeld) radiation boundary condition, $\dfrac{\partial u_o^e(\mu)}{\partial n_o} = \left(i\mu_{(3)} + \dfrac{1}{2R}\right) u_o^e(\mu)$, at the radiation boundary $\Gamma_{o,\text{R}}$; and we specify a Neumann boundary condition, $\partial u_o^e(\mu)/\partial n_o = 0$, on the horn wall $\Gamma_{o,\text{W}}$. We next specify the parameter domain $\mathcal{D} = [1.0, 1.8] \times [1.8, 2.5] \times [0, 2]$; we denote a particular parameter value as $\mu = (\mu_{(1)}, \mu_{(2)}, \mu_{(3)}) = (b_1, b_2, k) \in \mathcal{D}$, where k is the nondimensional frequency or wave number.

We now define our complex space $X_o^e = \{v = v_R + iv_I : v_R \in H^1(\Omega_o(\mu)), v_I \in H^1(\Omega_o(\mu))\}$. Let $\bar{v}$ denote the complex conjugate of v. We then specify, for all $\mu \in \mathcal{D}$ and for any $w, v \in X_o^e$, the sesquilinear form and anti-linear functional

$$\begin{aligned} a_o(w, v; \mu) &= (1 + i\epsilon) \int_{\Omega_o(\mu)} \nabla w \cdot \nabla \bar{v} - \mu_{(3)} \int_{\Omega_o(\mu)} w\bar{v} \\ &\quad + \int_{\Gamma_{o,\text{in}}} w\bar{v} + \left(\frac{1}{2R} + i\mu_{(3)}\right) \int_{\Gamma_{o,\text{R}}} w\bar{v}, \end{aligned} \tag{2.21}$$

$$f_o(v; \mu) = 2i\mu_{(3)} \int_{\Gamma_{o,\text{in}}} \bar{v}, \tag{2.22}$$

respectively. Here $\epsilon = 0.001$ represent a small dissipation in the medium. We also specify, for any $v \in X_o^e$, the output functional

$$\ell_o(v) = \int_{\Gamma_{o,\text{in}}} \bar{v}; \tag{2.23}$$

the output thus corresponds to a measurement of the pressure at the inlet $\Gamma_{o,\text{in}}$.

We then apply a domain decomposition technique (see [26]) to represent the bilinear and linear forms in our usual affine expansions: we divide $\Omega_o(\mu)$ into 20 subdomains and consider each subdomain as the image of a parameter independent "reference subdomain" under an affine transformation; we denote the union of these reference subdomains by Ω ($\equiv \Omega_o(\bar{\mu})$, where $\bar{\mu} = (1.4, 2.15, 0)$). We also introduce a space X^e such that any $v \in X^e$ maps to $v_o \in X_o^e$ through our piecewise affine transformation. The exact weak formulation for the pressure $u^e(\mu) \in X^e$ in the reference domain Ω is then given by a complex version of (2.5). Furthermore, through the domain decomposition technique we obtain complex versions of (2.1) and (2.2) for $Q_a = 25$ and $Q_f = 1$, respectively. We finally define, for all $w, v \in X^e$, our X-inner product for this problem as

$$(w, v)_X = \int_\Omega \nabla w \cdot \nabla \bar{v} + \int_\Omega w\bar{v}. \tag{2.24}$$

For our numerical results in Section 4.2.2 (focus calculations) and Section 5.4.2 (*hp*-RB approximations) we use for our truth calculations a standard $\mathbb{P}_1(\Omega)$ FE approximation space $X = X^{\mathcal{N}} \subset X^e$ of dimension $\mathcal{N} = 30108$, which is sufficiently accurate for our choice of frequency range. For purposes of illustration

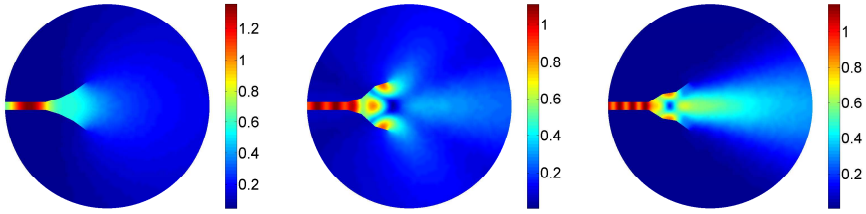

$\mu = [1.0, 1.8, 0.5]$ $\mu = [1.0, 2.5, 1.4]$ $\mu = [1.53, 1.8, 2.0]$

Figure 2.3: The magnitude of the pressure field in $\Omega_o(\mu)$ for different parameter values.

we show in Figure 2.3 three solution fields corresponding to different parameter values.

Although with the dissipation (and radiation) condition this problem is in fact coercive, it is preferable to consider for our *a posteriori* error estimators not a coercivity constant lower bound but rather an inf-sup constant lower bound β_{LB}: $0 < \beta_{\text{LB}}(\mu) \leq \beta(\mu)$. Here,

$$\beta(\mu) = \inf_{w \in X} \sup_{v \in X} \frac{|a(w, v; \mu)|}{\|w\|_X \|v\|_X}, \tag{2.25}$$

for all $\mu \in \mathcal{D}$, where $|\cdot|$ denotes complex modulus. Typically, this positive inf-sup lower bound is constructed by a natural norm version of the SCM procedure [16]. However, in this paper, for simplicity[1] we choose β_{LB} to be a constant: the minimum of the SCM lower bound over a dense set in $\mathcal{D}$. Admittedly, this choice will compromise both sharpness (since we invoke a minimum) and rigor (since this minimum is taken over a subset of $\mathcal{D}$) of our *a posteriori* error bound.

3 The Certified Derived Reduced Basis Method

In this section we introduce the new two-step RB method. For simplicity our development here is for coercive linear elliptic equations with real-valued fields. However, the extension to non-coercive equations and complex fields — required for our Helmholtz acoustic horn model problem — is straightforward.

3.1 Derived RB approximation

We introduce the intermediate (standard) RB approximation space $X_N \subset X$ of dimension $N \ll \mathcal{N}$. The space X_N is spanned by solutions of (2.7) for

[1] The natural-norm SCM procedure in [16] has a multi-parameter domain structure different from the multi-parameter domain structure of the *hp*-RB approach considered in this paper; a streamlined merger of these approaches is the subject of future work.

judiciously chosen (see Section 3.3) parameter values $\mu_1 \in \mathcal{D}, \ldots, \mu_N \in \mathcal{D}$,

$$X_N \equiv \text{span}\{u(\mu_1), \ldots, u(\mu_N)\} \equiv \text{span}\{\zeta_1, \ldots \zeta_N\}; \tag{3.1}$$

here, $\{\zeta_1, \ldots, \zeta_N\}$ denotes an X-orthonormal basis for X_N, obtained through (say) a modified Gram-Schmidt procedure.[2]

We may then introduce the RB approximation: given any $\mu \in \mathcal{D}$, find $u_N(\mu) \in X_N$ such that

$$a(u_N(\mu), v; \mu) = f(v; \mu), \quad \forall v \in X_N, \tag{3.2}$$

and then evaluate the RB output approximation as

$$s_N(\mu) = \ell(u_N(\mu)). \tag{3.3}$$

We now introduce a parameter subdomain or submanifold $\mathcal{D}' \subset \mathcal{D}$ to which the DRB model shall be specifically tailored. In the context of focus calculations, we wish to speed up evaluation of the RB solution, RB output, and RB error bound for any parameter value in the subdomain $\mathcal{D}' \subset \mathcal{D}$; in the context of *hp*-RB approximations, we wish to speedup evaluation of the RB solution, RB output, and RB error bound for any parameter value in $\mathcal{D}$ through a partition of $\mathcal{D}$ into *many* (K) subdomains $\mathcal{V}^k \subset \mathcal{D}$, $1 \le k \le K$ subdomains.[3] With regard to the *hp*-RB approximation, $\mathcal{D}'$ denotes in this section any of the K subdomains $\mathcal{V}^k$, $1 \le k \le K$; the *hp*-RB approximation is discussed in greater detail in Section 5.

We introduce the DRB approximation space $X_{N,M} \subset X_N$ of dimension $M \le N$. The space $X_{N,M}$ is spanned by solutions of (3.2) for judiciously chosen (see Section 3.3) parameter values $\mu'_1 \in \mathcal{D}', \ldots, \mu'_M \in \mathcal{D}'$,

$$X_{N,M} \equiv \text{span}\{u_N(\mu'_1), \ldots, u_N(\mu'_M)\} \equiv \text{span}\{\psi_1, \ldots \psi_M\}. \tag{3.4}$$

Here, $\{\psi_1, \ldots, \psi_M\}$ denotes an X-orthonormal basis for $X_{N,M}$, obtained through a Gram-Schmidt procedure; however we note that in practice, we shall not require the explicit ($\mathcal{N}$-dependent) computation of $\psi_1, \ldots, \psi_M$. The computational link between the intermediate and derived RB models will be discussed later in Section 3.4.

We may now finally introduce the DRB approximation: given any $\mu \in \mathcal{D}'$, find $u_{N,M}(\mu) \in X_{N,M}$ such that

$$a(u_{N,M}(\mu), v; \mu) = f(v; \mu), \quad \forall v \in X_{N,M}, \tag{3.5}$$

and then evaluate the DRB output approximation as

$$s_{N,M}(\mu) = \ell(u_{N,M}(\mu)). \tag{3.6}$$

[2] In the modified Gram-Schmidt procedure we compute $\tilde{\zeta}_i = u(\mu_i) - \sum_{n=1}^{i-1} (\zeta_n, u(\mu_i))_X \zeta_n$, $2 \le i \le N$, in an iterative fashion in order to preserve numerical stability in finite precision as described in [8]. Here $\zeta_1 = u(\mu_1)/\|u(\mu_1)\|_X$ and $\zeta_i = \frac{\tilde{\zeta}_i}{\|\tilde{\zeta}_i\|_X}$, $2 \le i \le N$.

[3] As described in the introduction, the DRB provides an *offline* (and not online *per se*) speedup of the *hp*-RB approximation. This offline speedup enlarges the class of problems amenable to RB treatment. However, this offline speedup may also accomodate larger K — smaller subdomains — and thus implicitly a speedup of the *hp*-RB online cost.

3.2 *A Posteriori* Error Estimation

We first recall the *a posteriori* error estimator for the (standard) RB approximation [26]. We define the residual

$$r_N(\cdot;\mu) = f(\cdot;\mu) - a(u_N(\mu),\cdot;\mu) \in X'; \tag{3.7}$$

we then introduce the Riesz representation of the residual, $\mathcal{R}_N(\mu) \in X$, which satisfies

$$(\mathcal{R}_N(\mu), v)_X = r_N(v;\mu), \quad \forall v \in X. \tag{3.8}$$

We may then define the RB error bound as[4]

$$\Delta_N(\mu) = \frac{\|\mathcal{R}_N(\mu)\|_X}{\alpha_{\rm LB}(\mu)}. \tag{3.9}$$

We may readily demonstrate that $\|u(\mu) - u_N(\mu)\|_X \le \Delta_N(\mu)$: We first note that the error $e_N(\mu) = u(\mu) - u_N(\mu)$ satisifes

$$a(e_N(\mu), v;\mu) = r_N(v;\mu), \quad \forall v \in X. \tag{3.10}$$

We then choose $v = e_N(\mu)$ and invoke (3.8) to obtain

$$a(e_N(\mu), e_N(\mu);\mu) = (\mathcal{R}_N(\mu), e_N(\mu))_X. \tag{3.11}$$

We apply coercivity to the left hand side and the Cauchy-Schwarz inequality to the right hand side to obtain

$$\alpha_{\rm LB}(\mu)\|e_N(\mu)\|_X^2 \le \|\mathcal{R}_N(\mu)\|_X \|e_N(\mu)\|_X, \tag{3.12}$$

from where we readily derive (3.9). We shall discuss the computation of $\Delta_N(\mu)$ — in particular the dual norm of the residual $\|\mathcal{R}_N(\mu)\|_X$ — in Section 3.4; however we note here that we may in the RB evaluation stage, for any given $\mu \in \mathcal{D}$, compute $\Delta_N(\mu)$ at cost $\mathcal{O}(Q^2N^2)$ — independently of the truth complexity $\mathcal{N}$.

The *a posteriori* error estimator for the DRB approximation is very similar. We define the residual

$$r_{N,M}(\cdot;\mu) = f(\cdot;\mu) - a(u_{N,M}(\mu),\cdot;\mu) \in X'; \tag{3.13}$$

we then introduce the Riesz representation of the residual, $\mathcal{R}_{N,M}(\mu) \in X$, which satisfies

$$(\mathcal{R}_{N,M}(\mu), v)_X = r_{N,M}(v;\mu), \quad \forall v \in X. \tag{3.14}$$

[4] We note that for our Helmholtz acoustic problem the RB error bound is given as in (3.9) with the coercivity constant lower bound $\alpha_{\rm LB}$ replaced by an inf-sup constant lower bound $\beta_{\rm LB}$.

We then define the error bound

$$\Delta_{N,M}(\mu) = \frac{\|\mathcal{R}_{N,M}(\mu)\|_X}{\alpha_{\rm LB}(\mu)}, \tag{3.15}$$

for which we may show that $\|u(\mu) - u_{N,M}(\mu)\|_X \leq \Delta_N(\mu)$ by arguments analogous to (3.10)–(3.12). We emphasize that $\Delta_{N,M}(\mu)$ bounds the error in the DRB approximation with respect to the truth upon which the *intermediate* RB model is built. We shall discuss the computation of $\Delta_{N,M}(\mu)$ in detail in Section 3.4; however we note here that we may in the DRB evaluation stage, for any given $\mu \in \mathcal{D}'$, compute $\Delta_{N,M}(\mu)$ at cost $\mathcal{O}(Q^2M^2)$ — independently of the truth complexity $\mathcal{N}$ *and* the RB complexity N.

For our sampling algorithm which we discuss in the next section we shall also require a bound for the error in the DRB approximation with respect to the intermediate RB approximation. We introduce the Riesz representation of the DRB residual in the RB space, $\tilde{\mathcal{R}}_{N,M}(\mu) \in X_N$, which satisfies

$$(\tilde{\mathcal{R}}_{N,M}(\mu), v)_X = r_{N,M}(v), \quad \forall v \in X_N. \tag{3.16}$$

We then define the error bound

$$\tilde{\Delta}_{N,M}(\mu) = \frac{\|\tilde{\mathcal{R}}_{N,M}(\mu)\|_X}{\alpha_{\rm LB}(\mu)}; \tag{3.17}$$

for which we may show that $\|u_N(\mu) - u_{N,M}(\mu)\|_X \leq \tilde{\Delta}_{N,M}(\mu)$ by arguments analogous to (3.10)–(3.12).

Finally, we note that we may readily develop error bounds for the RB (or DRB) output approximation. For example, for any $\mu \in \mathcal{D}$,

$$|s(\mu) - s_{N,M}(\mu)| = |\ell(u(\mu) - u_{N,M}(\mu))| \tag{3.18}$$

$$\leq \sup_{v \in X} \frac{\ell(v)}{\|v\|_X} \|u(\mu) - u_{N,M}(\mu)\|_X \tag{3.19}$$

$$\leq \|\ell\|_{X'} \Delta_{N,M}(\mu). \tag{3.20}$$

3.3 Greedy Parameter Sampling

For the construction of both the intermediate RB space X_N and the DRB space $X_{N,M}$, we invoke a Greedy parameter sampling procedure [26, 28], which we now discuss.

We first consider the construction of the intermediate RB approximation space. We introduce a training set $\Xi^{\mathcal{D}}_{\rm train} \subset \mathcal{D}$ of finite cardinality $|\Xi^{\mathcal{D}}_{\rm train}|$ which shall serve as a computational surrogate for $\mathcal{D}$. We then introduce as Algorithm 1 the Greedy$^{\rm RB}$ sampling procedure. For a specified tolerance $\epsilon^{\rm RB}_{\rm tol}$ and an initial parameter value $\mu_1 \in \mathcal{D}$, Algorithm 1 returns a space $X_{N_{\max}} \subset X$ of dimension $N_{\max}$ such that $\Delta_{N_{\max}}(\mu) \leq \epsilon^{\rm RB}_{\rm tol}$ for all $\mu \in \Xi^{\mathcal{D}}_{\rm train}$. We typically choose $\Xi^{\mathcal{D}}_{\rm train}$ "dense" and hence we may anticipate that $\Delta_{N_{\max}}(\mu) \leq \epsilon^{\rm RB}_{\rm tol}$ for most $\mu \in \mathcal{D}$. We note that due to the hierarchical structure of the spaces —

Algorithm 1 $X_{N_{\max}} = \text{Greedy}^{\text{RB}}(\mu_1, \epsilon_{\text{tol}}^{\text{RB}})$

$N \leftarrow 1$
$X_N = \text{span}\{u(\mu_N)\}$
$\epsilon_N^{\max} = \max_{\mu \in \Xi_{\text{train}}^{\mathcal{D}}} \Delta_N(\mu)$
while $\epsilon_N^{\max} > \epsilon_{\text{tol}}^{\text{RB}}$ **do**
  $N \leftarrow N + 1$
  $\mu_N = \arg\max_{\mu \in \Xi_{\text{train}}^{\mathcal{D}}} \Delta_{N-1}(\mu)$
  $X_N = X_{N-1} \oplus \text{span}\{u(\mu_N)\}$
  $\epsilon_N^{\max} = \max_{\mu \in \Xi_{\text{train}}^{\mathcal{D}}} \Delta_N(\mu)$
end while
$N_{\max} = N$

Algorithm 2 $X_{N,M_{\max}} = \text{Greedy}^{\text{DRB}}(\mu_1', N, \epsilon_{\text{tol}}^{\text{DRB}})$

$M \leftarrow 1$
$X_{N,M} = \text{span}\{u(\mu_M')\}$
$\epsilon_{N,M}^{\max} = \max_{\mu \in \Xi_{\text{train}}^{\mathcal{D}'}} \tilde{\Delta}_{N,M}(\mu)$
while $\epsilon_{N,M}^{\max} > \epsilon_{\text{tol}}^{\text{DRB}}$ **do**
  $M \leftarrow M + 1$
  $\mu_M' = \arg\max_{\mu \in \Xi_{\text{train}}^{\mathcal{D}'}} \tilde{\Delta}_{N,M-1}(\mu)$
  $X_{N,M} = X_{N,M-1} \oplus \text{span}\{u_N(\mu_M')\}$
  $\epsilon_M^{\max} = \max_{\mu \in \Xi_{\text{train}}^{\mathcal{D}'}} \tilde{\Delta}_{N,M}(\mu)$
end while
$M_{\max} = M$

$X_1 \subset \cdots \subset X_{N_{\max}}$ — we may readily extract spaces of dimension $N < N_{\max}$ from $X_{N_{\max}}$.

We next consider the construction of the DRB approximation space. We introduce a training set $\Xi^{\mathcal{D}'}_{\text{train}} \subset \mathcal{D}'$ ($\subset \mathcal{D}$) of finite cardinality $|\Xi^{\mathcal{D}'}_{\text{train}}|$ which shall serve as our computational surrogate for $\mathcal{D}'$. We then introduce as Algorithm 2 the Greedy$^{\text{DRB}}$ sampling procedure. For a specified tolerance $\epsilon^{\text{DRB}}_{\text{tol}}$, a desired intermediate RB space (upon which the DRB space is built) dimension $N \leq N_{\max}$, and an initial parameter value $\mu'_1 \in \mathcal{D}'$, Algorithm 2 returns a space $X_{N,M_{\max}} \subseteq X_N$ of dimension $M_{\max} \leq N$ such that $\tilde{\Delta}_{N,M_{\max}}(\mu) \leq \epsilon^{\text{DRB}}_{\text{tol}}$ for all $\mu \in \Xi^{\mathcal{D}'}_{\text{train}}$. We note that due to the hierarchical structure of the spaces — $X_{N,1} \subset \cdots \subset X_{1,M_{\max}}$ — we may readily extract spaces of dimension $M < M_{\max}$ from $X_{N,M_{\max}}$. We emphasize that Algorithm 2 is identical to Algorithm 1 except for the procedures for snapshot computation and error bound evaluation.

We note that in Algorithm 2 we invoke the error bound (3.17) with respect to the intermediate RB approximation in order to ensure convergence of the algorithm: the maximum error bound $\epsilon^{\max}_{N,M} \to 0$ as $M \to N$ and hence any specified tolerance $\epsilon^{\text{DRB}}_{\text{tol}} > 0$ will eventually be satisfied. We also note that, for any $\mu \in \Xi^{\mathcal{D}'}_{\text{train}}$, the error in the DRB approximation with respect to the truth can be bounded as

$$\begin{aligned}\|u(\mu) - u_{N,M}(\mu)\|_X &\leq \|u(\mu) - u_N(\mu)\|_X + \|u_N(\mu) - u_{N,M}(\mu)\|_X \\ &\leq \Delta_N(\mu) + \tilde{\Delta}_{N,M}(\mu) \leq \epsilon^{\max}_N + \epsilon^{\max}_{N,M}. \quad (3.21)\end{aligned}$$

However, we can not reduce the term $\epsilon^{\max}_N$ since we increase only M (and not N) during the Greedy$^{\text{DRB}}$ sampling procedure. As a result we typically choose in practice $\epsilon^{\text{DRB}}_{\text{tol}} > \epsilon^{\text{RB}}_{\text{tol}}$ in order to avoid Greedy$^{\text{DRB}}$ iterations that do not provide significant error (with respect to the truth) reduction.

We emphasize that in the online stage we bound the error in the DRB approximation with respect to the truth. We note that in practice we do not invoke $\Delta_N(\mu) + \tilde{\Delta}_{N,M}(\mu)$ (in (3.21)) as an error bound, since evaluation of $\Delta_N(\mu)$ is expensive (N-dependent). We thus invoke in the online stage the less expensive (evaluation cost depends on M, and not on N) bound $\Delta_{N,M}(\mu)$ in (3.15). We discuss computational procedures and associated computational cost next.

3.4 Construction-Evaluation Computational Procedures

The key ingredients in our computational procedures are the affine expansions (2.1) and (2.2) of a and f, respectively. The construction–evaluation procedures which we introduce here enable efficient offline–online computational procedures. We discuss application of the construction–evaluation procedures to the offline–online decoupling for each of our two particular applications, focus calculation and *hp*-RB approximation, in Section 4 and Section 5, respectively.

3.4.1 Output Approximation

RB output. We first expand the RB field approximation in terms of the basis functions $\zeta_1, \ldots, \zeta_N$ of X_N as

$$u_N(\mu) = \sum_{n=1}^{N} u_{N,n}(\mu)\zeta_n. \tag{3.22}$$

With (2.1) and (2.2) we may then write (3.2) as the linear system

$$\sum_{j=1}^{N} u_{N,j}(\mu)\left(\sum_{q=1}^{Q_a} a^q(\zeta_j,\zeta_i)\Theta_a^q(\mu)\right) = \sum_{q=1}^{Q_f} f^q(\zeta_i)\Theta_f^q(\mu), \quad 1 \le i \le N, \tag{3.23}$$

in the coefficients $u_{N,j}(\mu)$, $1 \le j \le N$. We obtain the RB output approximation (3.3) as

$$s_N(\mu) = \ell(u_N(\mu)) = \sum_{n=1}^{N} u_{N,n}(\mu)\ell(\zeta_n). \tag{3.24}$$

We now identify the construction and evaluation stages. In the construction stage we compute for $1 \le q \le Q_a$ the "stiffness matrices" $A_N^q \equiv \{a^q(\zeta_j,\zeta_i)\} \in \mathbb{R}^{N\times N}$; we compute for $1 \le q \le Q_f$ the "load vectors" $F_N^q \equiv \{f^q(\zeta_i)\} \in \mathbb{R}^N$; we also compute the terms $\ell(\zeta_i)$ $(1 \le i \le N)$ required for the output. The construction stage is performed at cost $\mathcal{O}(\mathcal{N}^\bullet)$. In the evaluation stage, given any $\mu \in \mathcal{D}$, we evaluate $\Theta_a^q(\mu)$, $1 \le q \le Q_a$, and $\Theta_f^q(\mu)$, $1 \le q \le Q_f$, at cost $\mathcal{O}(Q)$; we then perform the two summations over q in (3.23) at cost $\mathcal{O}(Q_a N^2 + Q_f N)$, and solve the $N \times N$ linear system for the RB coefficients $u_{N,n}(\mu)$, $1 \le n \le N$, at cost $\mathcal{O}(N^3)$ (we must anticipate that the RB system matrix is dense). We finally evaluate the RB output approximation (3.24) at cost $\mathcal{O}(N)$.

DRB output. We first expand the basis functions $\psi_1, \ldots, \psi_M$ of $X_{N,M}$ in terms of the basis functions $\zeta_1, \ldots, \zeta_N$ of X_N as

$$\psi_i = \sum_{n=1}^{N} \kappa_{i,n}\zeta_n, \quad 1 \le i \le M; \tag{3.25}$$

recall that

$$\underbrace{\text{span}\{\psi_1, \ldots, \psi_M\}}_{X_{N,M}} = \underbrace{\text{span}\{u_N(\mu_1'), \ldots, u_N(\mu_M')\}}_{X_{N,M}} \subset \underbrace{\text{span}\{\zeta_1, \ldots, \zeta_N\}}_{X_N}, \tag{3.26}$$

where $\psi_1, \ldots, \psi_M$ is an X-orthonormal basis for $X_{N,M}$. We may obtain the coefficients $\kappa_{m,n}$, $1 \le m \le M$, $1 \le n \le N$, from the Gram-Schmidt procedure

for $\psi_1, \ldots, \psi_M$ as follows. For $m = 1$, we obtain

$$\psi_1 = \frac{u_N(\mu_1')}{\|u_N(\mu_1')\|_X} = \frac{\sum_{n=1}^N u_{N,n}(\mu_1')\zeta_n}{\Big(\sum_{m=1}^N \sum_{n=1}^N u_{N,n}(\mu_1') u_{N,m}(\mu_1') \underbrace{(\zeta_m, \zeta_n)_X}_{\delta_{m,n}}\Big)^{1/2}} \tag{3.27}$$

$$= \frac{\sum_{n=1}^N u_{N,n}(\mu_1')\zeta_n}{\Big(\sum_{n=1}^N (u_{N,n}(\mu_1'))^2\Big)^{1/2}} \equiv \sum_{n=1}^N \kappa_{1,n}\zeta_n, \tag{3.28}$$

where $\delta_{i,j}$ is the Kroenecker delta symbol. For $2 \le m \le M$, we further obtain $\psi_m = \tilde{\psi}_m / \|\tilde{\psi}_m\|_X$ where, from (3.22) and (3.25),

$$\tilde{\psi}_m = u_N(\mu_m') - \sum_{s=1}^{m-1} (\psi_s, u_N(\mu_m'))_X \psi_s, \tag{3.29}$$

$$= \sum_{n=1}^N u_{N,n}(\mu_m')\zeta_n - \sum_{s=1}^{m-1}\sum_{n=1}^N \sum_{k=1}^N \sum_{l=1}^N u_{N,l}(\mu_m')\kappa_{s,k} \underbrace{(\zeta_k, \zeta_l)_X}_{\delta_{k,l}} \kappa_{s,n}\zeta_n \tag{3.30}$$

$$= \sum_{n=1}^N \Big(u_{N,n}(\mu_m') - \sum_{s=1}^{m-1}\sum_{k=1}^N u_{N,k}(\mu_m')\kappa_{s,k}\kappa_{s,n}\Big)\zeta_n \equiv \sum_{n=1}^N \tilde{\kappa}_{m,n}\zeta_n. \tag{3.31}$$

We thus identify $\kappa_{m,n} = \tilde{\kappa}_{m,n}/\|\tilde{\psi}_m\|_X$, $1 \le n \le N$, with

$$\|\tilde{\psi}_m\|_X = \Big(\sum_{n=1}^N \sum_{k=1}^N \tilde{\kappa}_{m,n}\tilde{\kappa}_{m,k} \underbrace{(\zeta_n, \zeta_k)_X}_{\delta_{n,k}}\Big)^{1/2} \tag{3.32}$$

$$= \Big(\sum_{n=1}^N \tilde{\kappa}_{m,n}^2\Big)^{1/2}. \tag{3.33}$$

In practice, we do not explicitly perform this ($\mathcal{N}$-dependent) Gram-Schmidt procedure since we do not explicitly require the DRB basis functions ψ_m, $1 \le m \le M$. From (3.28), (3.31), and (3.33), we obtain the coefficients $\kappa_{m,n}$ at cost $\mathcal{O}(NM^2)$ (we use a sum-factorization technique in (3.31)).[5]

We next expand the DRB field approximation in terms of the basis functions of $X_{N,M}$ as

$$u_{N,M}(\mu) = \sum_{m=1}^M u_{N,M,m}(\mu)\psi_m. \tag{3.34}$$

[5]In (3.28), (3.31), and (3.33) we invoke the fact that $(\zeta_k, \zeta_l)_X = \delta_{k,l}$; however this is only true in infinite precision. An improvement to the numerical stability of our approach is thus to compute and store $(\zeta_k, \zeta_l)_X$, $1 \le k, l \le N$; we may then obtain $\kappa_{1,n}$ from (3.27) rather than from (3.28), and $\tilde{\kappa}_{m,n}$ and $\|\tilde{\psi}_m\|_X$, $2 \le m \le M$, from (3.30) and (3.32) rather than from (3.31) and (3.33), respectively. Note (3.30) requires $\mathcal{O}(N^2M)$ operations but (3.31) only $\mathcal{O}(NM^2)$.

With (2.1) and (2.2) we may then write (3.5) as the linear system

$$\sum_{j=1}^{M} u_{N,M,j}(\mu)\left(\sum_{q=1}^{Q_a} a^q(\psi_j,\psi_i)\Theta_a^q(\mu)\right) = \sum_{q=1}^{Q_f} f^q(\psi_i)\Theta_f^q(\mu), \quad 1 \le i \le M \quad (3.35)$$

in the coefficients $u_{N,M,j}(\mu)$, $1 \le j \le M$. We obtain the DRB output approximation (3.6) as

$$s_{N,M}(\mu) = \ell(u_{N,M}(\mu)) = \sum_{m=1}^{M} u_{N,M,m}(\mu)\ell(\psi_m). \quad (3.36)$$

With (3.25), we note that we may write $a^q(\psi_j,\psi_i)$, $f^q(\psi_i)$, and $\ell(\psi_i)$ as

$$a^q(\psi_j,\psi_i) = \sum_{n=1}^{N} \kappa_{j,n}\left(\sum_{m=1}^{N} \kappa_{i,m} a^q(\zeta_n,\zeta_m)\right), \quad 1 \le q \le Q_a, \quad 1 \le i,j \le M, \quad (3.37)$$

$$f^q(\psi_i) = \sum_{n=1}^{N} \kappa_{i,n} f^q(\zeta_n), \qquad 1 \le q \le Q_f, \quad 1 \le i \le M, \quad (3.38)$$

$$\ell(\psi_i) = \sum_{n=1}^{N} \kappa_{i,n}\ell(\zeta_n), \qquad 1 \le i \le M, \quad (3.39)$$

respectively. We may then identify the construction and evaluation stages. In the construction stage we first obtain, for $1 \le q \le Q_a$, the matrices $A_{N,M}^q \equiv \{a^q(\psi_j,\psi_i)\} \in \mathbb{R}^{M\times M}$ from the matrices $A_N^q \in \mathbb{R}^{N\times N}$ by (3.37) at cost $\mathcal{O}(N^2M)$ through a sum factorization technique as follows: for $1 \le q \le Q_a$, we first compute and store (temporarily) the terms

$$\tau_{i,n}^q = \sum_{m=1}^{N} \kappa_{i,m} a^q(\zeta_n,\zeta_m), \qquad 1 \le i \le M, \quad 1 \le n \le N, \quad (3.40)$$

at cost $\mathcal{O}(N^2M)$; we then perform the outer summation

$$a^q(\psi_j,\psi_i) = \sum_{n=1}^{N} \kappa_{j,n}\tau_{i,n}^q, \qquad 1 \le i,j \le M, \quad (3.41)$$

at cost $\mathcal{O}(M^2N)$. The total cost of (3.37) is thus $\mathcal{O}(N^2M)$ (for each q) since $M \le N$.

We next obtain, for $1 \le q \le Q_f$, the vectors $F_{N,M}^q \equiv \{f^q(\psi_i)\} \in \mathbb{R}^M$ from the vectors $F_N^q \in \mathbb{R}^N$ by (3.38) at cost $\mathcal{O}(MN)$; and we obtain $\ell(\psi_i)$, $1 \le i \le M$, from $\ell(\zeta_n)$, $1 \le n \le N$, by (3.39) at cost $\mathcal{O}(MN)$. The cost of the construction stage is thus $\mathcal{N}$-independent. In the evaluation stage, given any $\mu \in \mathcal{D}'$, we evaluate $\Theta_a^q(\mu)$, $1 \le q \le Q_a$, and $\Theta_f^q(\mu)$, $1 \le q \le Q_f$, at cost $\mathcal{O}(Q)$; we then perform the two summations over q in (3.35) at cost $\mathcal{O}(Q_aM^2 + Q_fM)$, and solve the $M \times M$ linear system for the DRB coefficients $u_{N,M,m}(\mu)$, $1 \le m \le M$, at cost $\mathcal{O}(M^3)$. We finally evaluate the DRB output approximation (3.36) at cost $\mathcal{O}(M)$.

3.4.2 *A Posteriori* Error Bound

We discuss here the computational procedures associated with the residual dual norms required for our *a posteriori* error estimators. We refer to [16, 17, 26] for the computational procedures associated with the coercivity (or stability factor) lower bound (the SCM).

Dual X-norm of RB residual. We now discuss the construction-evaluation procedure for the dual norm of the RB residual. With (2.1), (2.2), and (3.22), we may expand (3.8) as

$$(\mathcal{R}_N(\mu), v)_X = \sum_{q=1}^{Q_f} f^q(v)\Theta_q^f(\mu) - \sum_{n=1}^{N} u_{N,n}(\mu) \sum_{q=1}^{Q_a} a^q(\zeta_n, v)\Theta_a^q(\mu) \tag{3.42}$$

$$= \sum_{i=1}^{\bar{N}} \phi^i(\mu)\mathcal{L}^i(v), \tag{3.43}$$

for all $v \in X$. Here $\bar{N} = Q_f + NQ_a$, and the $\mathcal{L}^i \in X'$ and $\phi^i : \mathcal{D} \to \mathbb{R}$ are defined explicitly as

$$\mathcal{L}^i = f^i, \qquad 1 \le i \le Q_f, \tag{3.44}$$

$$\mathcal{L}^{Q_f+i+(n-1)Q_a} = a^i(\zeta_n, \cdot), \qquad 1 \le i \le Q_a, \quad 1 \le n \le N, \tag{3.45}$$

$$\phi^i = \Theta_f^i, \qquad 1 \le i \le Q_f, \tag{3.46}$$

$$\phi^{Q_f+i+(n-1)Q_a} = u_{N,n}\Theta_a^i, \qquad 1 \le i \le Q_a, \quad 1 \le n \le N. \tag{3.47}$$

We then define $l^i \in X$, $1 \le i \le \bar{N}$, such that

$$(l^i, v)_X = \mathcal{L}^i(v), \quad \forall v \in X. \tag{3.48}$$

Hence, by linearity,

$$\mathcal{R}_N(\mu) = \sum_{i=1}^{\bar{N}} \phi^i(\mu) l^i. \tag{3.49}$$

We may now identify the construction and evaluation stages. In the construction stage we solve (3.48), $1 \le i \le \bar{N}$, and compute the inner products $(l^i, l^j)_X$, $1 \le i, j \le \bar{N}$, at cost $\mathcal{O}(\mathcal{N}^\bullet)$. In the evaluation stage, given the RB solution coefficents for any $\mu \in \mathcal{D}$, we evaluate $\phi^i(\mu)$, $1 \le i \le \bar{N}$, at cost $\mathcal{O}(Q_f + Q_a N)$, and perform the summation

$$\|\mathcal{R}_N(\mu)\|_X^2 = \sum_{i=1}^{\bar{N}} \sum_{j=1}^{\bar{N}} \phi^i(\mu)\phi^j(\mu)(l^i, l^j)_X, \tag{3.50}$$

at cost $\mathcal{O}(\bar{N}^2) = \mathcal{O}(Q^2 N^2)$.

Dual X-norm of DRB residual. We next discuss the construction-evaluation procedure for the dual norm of the DRB residual. With (2.1), (2.2), and (3.34), we may expand (3.14) as

$$(\mathcal{R}_{N,M}(\mu), v)_X = \sum_{q=1}^{Q_f} f^q(v)\Theta_q^f(\mu) - \sum_{m=1}^{M} u_{N,M,m}(\mu) \sum_{q=1}^{Q_a} a^q(\psi_m, v)\Theta_a^q(\mu) \quad (3.51)$$

$$= \sum_{i=1}^{\bar{M}} \varphi^i(\mu)\mathcal{H}^i(v), \quad (3.52)$$

for all $v \in X$. Here $\bar{M} = Q_f + MQ_a$, and the $\mathcal{H}^i \in X'$ and $\varphi^i : \mathcal{D}' \to \mathbb{R}$ are defined explicitly as

$$\mathcal{H}^i = f^i, \qquad 1 \le i \le Q_f, \quad (3.53)$$

$$\mathcal{H}^{Q_f+i+(m-1)Q_a} = a^i(\psi_m, \cdot), \qquad 1 \le i \le Q_a, \quad 1 \le m \le M, \quad (3.54)$$

$$\varphi^i = \Theta_f^i, \qquad 1 \le i \le Q_f, \quad (3.55)$$

$$\varphi^{Q_f+i+(m-1)Q_a} = u_{N,M,m}\Theta_a^i, \qquad 1 \le i \le Q_a, \quad 1 \le m \le M. \quad (3.56)$$

We then define $h^i \in X$, $1 \le i \le \bar{M}$, such that

$$(h^i, v)_X = \mathcal{H}^i(v), \quad \forall v \in X. \quad (3.57)$$

Hence, by linearity,

$$\mathcal{R}_{N,M}(\mu) = \sum_{i=1}^{\bar{M}} \varphi^i(\mu) h^i. \quad (3.58)$$

We now note, by (3.25), that we may further expand the $\mathcal{H}^{Q_f+i+(m-1)Q_a}$ in (3.54) in terms of the intermediate RB basis $\{\zeta_n\}_{n=1}^N$ as

$$\mathcal{H}^{Q_f+i+(m-1)Q_a} = a^i(\psi_m, \cdot) = \sum_{n=1}^{N} \kappa_{m,n} a^i(\zeta_n, \cdot), \quad (3.59)$$

for $1 \le i \le Q_a$ and $1 \le m \le M$; thus, by linearity,

$$h^{Q_f+i+(m-1)Q_a} = \sum_{n=1}^{N} \kappa_{m,n} l^{Q_f+i+(n-1)Q_a}, \quad (3.60)$$

for $1 \le i \le Q_a$ and $1 \le m \le M$. We recall the definition of l^i, $1 \le i \le Q_f + NQ_a$, from (3.48), (3.44), and (3.45).

We next consider the inner products $(h^i, h^j)_X$, $1 \le i, j \le \bar{M}$. First, it is clear that

$$(h^i, h^j)_X = (l^i, l^j)_X, \quad 1 \le i, j \le Q_f; \quad (3.61)$$

further, we note that

$$(h^{Q_f+i+(m-1)Q_a}, h^j)_X = \sum_{n=1}^{N} \kappa_{m,n} (l^{Q_f+i+(n-1)Q_a}, l^j)_X, \tag{3.62}$$

$$(h^j, h^{Q_f+i+(m-1)Q_a})_X = \sum_{n=1}^{N} \kappa_{m,n} (l^j, l^{Q_f+i+(n-1)Q_a})_X, \tag{3.63}$$

for $1 \le i \le Q_a$, $1 \le m \le M$, and $1 \le j \le Q_f$; we finally note that

$$\begin{aligned}(h^{Q_f+i+(m-1)Q_a}, h^{Q_f+j+(m'-1)Q_a})_X \\ = \sum_{n=1}^{N} \kappa_{m,n} \left(\sum_{n'=1}^{N} \kappa_{m',n'} (l^{Q_f+i+(n-1)Q_a}, l^{Q_f+j+(n'-1)Q_a})_X \right),\end{aligned} \tag{3.64}$$

for $1 \le i, j \le Q_a$, $1 \le m, m' \le M$. The key observation here is that once $(l^i, l^j)_X$, $1 \le i, j \le \bar{N}$, are given from the intermediate RB construction stage, the analogous data $(h^i, h^j)_X$, $1 \le i, j \le \bar{M}$, for the DRB model may be obtained at cost $\mathcal{O}(N^\bullet)$ — independently of the truth complexity $\mathcal{N}$.

We may now identify the construction and evaluation stages. In the construction stage we obtain $(h^i, h^j)_X$, $1 \le i, j \le \bar{M}$, from $(l^i, l^j)_X$, $1 \le i, j \le \bar{N}$, by (3.61)–(3.64). The cost is dominated by the summation (3.64), for which we invoke a sum factorization technique: we first compute and store the term in parentheses for $1 \le i, j \le Q_a$, $1 \le n \le N$ and $1 \le m' \le M$ at cost $\mathcal{O}(Q_a^2 N^2 M)$; we then perform the outer summation (over n) for $1 \le i, j$ and $1 \le m, m' \le M$ at cost $\mathcal{O}(Q_a^2 M^2 N)$. The total cost is thus $\mathcal{O}(Q_a^2 N^2 M)$ since $M \le N$. (Direct evaluation of (3.64) requires $\mathcal{O}(Q^2 N^2 M^2)$ operations.) In particular, the DRB construction stage is $\mathcal{N}$-independent. In the evaluation stage, given the DRB solution coefficents for any $\mu \in \mathcal{D}'$, we evaluate $\varphi^i(\mu)$, $1 \le i \le \bar{M}$, at cost $\mathcal{O}(\bar{M}) = \mathcal{O}(Q_f + Q_a M)$, and perform the summation

$$\|\mathcal{R}_{N,M}(\mu)\|_X^2 = \sum_{i=1}^{\bar{M}} \sum_{j=1}^{\bar{M}} \varphi^i(\mu) \varphi^j(\mu) (h^i, h^j)_X \tag{3.65}$$

at cost $\mathcal{O}(\bar{M}^2) = \mathcal{O}(Q^2 M^2)$.

Dual X_N-norm of DRB residual. We next discuss the construction-evaluation procedure for the dual norm of the DRB residual with respect to the intermediate RB approximation space, $\|\tilde{\mathcal{R}}_{N,M}(\mu)\|_X$. With (2.1), (2.2), and (3.34), we may expand (3.16) as

$$(\tilde{\mathcal{R}}_{N,M}(\mu), v)_X = \sum_{q=1}^{Q_f} f^q(v) \Theta_q^f(\mu) - \sum_{m=1}^{M} u_{N,M,m}(\mu) \sum_{q=1}^{Q_a} a^q(\psi_m, v) \Theta_a^q(\mu) \tag{3.66}$$

$$= \sum_{i=1}^{\bar{M}} \varphi^i(\mu) \mathcal{H}^i(v), \tag{3.67}$$

for all $v \in X_N$. We then define $\tilde{h}^i \in X_N$, $1 \le i \le \bar{M}$, such that

$$(\tilde{h}^i, v)_X = \mathcal{H}^i(v), \quad \forall v \in X_N. \tag{3.68}$$

Hence, by linearity,

$$\tilde{\mathcal{R}}_{N,M}(\mu) = \sum_{i=1}^{\bar{M}} \varphi^i(\mu)\tilde{h}^i. \tag{3.69}$$

We next consider the inner products $(\tilde{h}^i, \tilde{h}^j)_X$, $1 \le i, j \le \bar{M}$. We note that $\tilde{h}^i \in X_N$ may be written as

$$\tilde{h}^i = \sum_{n=1}^{N} \eta_n^i \zeta_n, \quad 1 \le i \le \bar{M}, \tag{3.70}$$

where the coefficients $\eta_1^i, \ldots, \eta_N^i$ satisfy

$$\sum_{n=1}^{N} \eta_n^i \underbrace{(\zeta_n, \zeta_m)_X}_{\delta_{m,n}} = \eta_m^i = \mathcal{H}^i(\zeta_m), \quad 1 \le m \le N, \tag{3.71}$$

thanks to the X-orthonormal basis for X_N. Hence

$$(\tilde{h}^i, \tilde{h}^j)_X = \sum_{m=1}^{N}\sum_{n=1}^{N} \eta_m^i \eta_n^j \underbrace{(\zeta_m, \zeta_n)_X}_{\delta_{m,n}} = \sum_{n=1}^{N} \mathcal{H}^i(\zeta_n)\mathcal{H}^j(\zeta_n), \tag{3.72}$$

for $1 \le i, j \le \bar{M}$.

We may now identify the construction and evaluation stages. In the construction stage we compute the inner products $(\tilde{h}^i, \tilde{h}^j)_X$, $1 \le i, j \le \bar{M}$, from (3.72) at cost $\mathcal{O}(N\bar{M}^2)$; note that $\mathcal{H}^i(\zeta_n)$, $1 \le i \le \bar{M}$, $1 \le n \le N$, may be evaluated from (3.53) and (3.59) at cost $\mathcal{O}(N^2\bar{M})$ since the matrices A_N^q, $1 \le q \le Q_a$, and vectors F_N^q, $1 \le q \le Q_f$, are computed and stored during the construction stage for the intermediate RB output. In the evaluation stage, given the DRB solution coefficients for any $\mu \in \mathcal{D}$, we evaluate $\varphi^i(\mu)$, $1 \le i \le \bar{M}$, at cost $\mathcal{O}(Q_f + Q_a M)$, and perform the summation

$$\|\tilde{\mathcal{R}}_{N,M}(\mu)\|_X^2 = \sum_{i=1}^{\bar{M}}\sum_{j=1}^{\bar{M}} \varphi^i(\mu)\varphi^j(\mu)(\tilde{h}^i, \tilde{h}^j)_X, \tag{3.73}$$

at cost $\mathcal{O}(\bar{M}^2) = \mathcal{O}(Q^2M^2)$.

We note that as an alternative to the bound $\tilde{\Delta}_{N,M}(\mu)$ we may directly compute $\|u_N(\mu) - u_{N,M}(\mu)\|_X$ at cost $\mathcal{O}(QN^2 + N^3)$. However typically M is significantly smaller than N and thus computation of $\tilde{\Delta}_{N,M}(\mu)$ is typically less expensive than computation of $\|u_N(\mu) - u_{N,M}(\mu)\|_X$ when the bound is required for many μ as in the Greedy$^{\text{DRB}}$ algorithm.

4 Focus Calculations

In the context of focus calculations we require many (or real-time) RB output (or RB error bound) evaluations over a parameter subset or submanifold $\mathcal{D}' \subset \mathcal{D}$. Given an intermediate RB model developed for the parameter domain $\mathcal{D}$, a smaller DRB model is typically sufficient over $\mathcal{D}' \subset \mathcal{D}$. This smaller DRB model may yield significant speedup compared to the standard RB alternative while preserving numerical accuracy.

4.1 Offline–Online Decomposition

We now discuss the offline-online decomposition associated with the focus calculation context. The *offline* stage is the construction of the intermediate RB model over $\mathcal{D}$: we perform Greedy$^{\text{RB}}$ (Algorithm 1) for a specified initial parameter value $\mu_1 \in \mathcal{D}$ and a specified error bound tolerance $\epsilon_{\text{tol}}^{\text{RB}}$ (to be satisfied over the training set $\Xi_{\text{train}}^{\mathcal{D}} \subset \mathcal{D}$). This stage is expensive — the cost is $\mathcal{O}(\mathcal{N}^\bullet)$ — but performed only once as preprocessing.

In the *online* stage, given a parameter subdomain or submanifold $\mathcal{D}' \subset \mathcal{D}$, we first construct the DRB model: we perform Greedy$^{\text{DRB}}$ (Algorithm 2) for a specified initial parameter value $\mu_1' \in \mathcal{D}'$, a specified intermediate RB space (constructed offline and upon which the DRB approximation is built) dimension $N \leq N_{\max}$, and a specified error bound tolerance $\epsilon_{\text{tol}}^{\text{DRB}}$ (to be satisfied over the training set $\Xi_{\text{train}}^{\mathcal{D}'} \subset \mathcal{D}'$). The cost of this step derives from RB snapshot computation and RB error bound preprocessing and evaluation; below $\bar{M}_{\max} \equiv Q_f + Q_a M_{\max}$.

1. RB snapshot computation. We compute $M_{\max}$ intermediate RB snapshots of complexity $N_{\max}$. The cost is $\mathcal{O}(M_{\max}(QN_{\max}^2 + N_{\max}^3))$ (we must anticipate that the RB system is dense).

2. DRB construction. We obtain the parameter independent matrices and vectors associated with the DRB system at cost $\mathcal{O}(QN_{\max}^2 M_{\max})$; note that we obtain these entities directly from the respective intermediate RB entities (computed offline).

3. DRB error bound preprocessing. We must compute $\bar{M}_{\max}^2$ inner products (3.72) for our error bound $\tilde{\Delta}_{N,M}$ (used in the Greedy$^{\text{DRB}}$ sampling procedure) and $\bar{M}_{\max}^2$ inner products (3.61)–(3.64) for our error bound $\Delta_{N,M}$ (used for DRB output certification). The total cost is dominated by (3.64) and is $\mathcal{O}(Q^2 N_{\max}^2 M_{\max})$.

4. DRB error bound evaluation. We compute the DRB approximation and evaluate the DRB error bound $\tilde{\Delta}_{N,M}$ over the training set $\Xi_{\text{train}}^{\mathcal{D}'}$ at each Greedy$^{\text{DRB}}$ iteration. The cost is, to leading order, $\mathcal{O}(M_{\max}|\Xi_{\text{train}}^{\mathcal{D}'}|(M_{\max}^3 + M_{\max}^2 Q^2))$.

5. DRB focus calculations. For any new parameter value $\mu \in \mathcal{D}'$ and given $1 \leq M \leq M_{\max}$, we perform DRB evaluation: computation of the DRB

solution, DRB output, and DRB error bound with respect to the truth approximation at cost $\mathcal{O}(M^3 + M^2Q^2)$.

Note that the focus calculation online stage includes the construction of the DRB model over $\mathcal{D}'$ — steps 1-4 above. The key point is that this DRB model is built inexpensively ($\mathcal{N}$-independently) upon the underlying intermediate RB model; the subsequent DRB evaluation stage (step 5 above, performed many times over $\mathcal{D}'$) is then independent of $\mathcal{N}$ *and* N. As a result, in the many-query context, a DRB approach may provide significant speedup compared to the standard RB alternative.

We finally note the important role of the sum factorization invoked in (3.37) and (3.64). The complexity reduction — a factor of M — is significant in practice in particular for focus calculations since the calculations (3.37) and (3.64) are performed online.

4.2 Numerical Results

4.2.1 Thermal Block

We develop a DRB approximation for the thermal block problem introduced in Section 2.2.1 in order to accelerate a focus calculation. We first generate an intermediate RB approximation of dimension $N_{\max} = 96$: we perform Greedy$^{\text{RB}}$ for $\mu_1 = (0.75, 0.75)$ and $\epsilon_{\text{tol}}^{\text{RB}} = 10^{-4}$ over a uniformly distributed random training set $\Xi_{\text{train}}^{\mathcal{D}} \subset \mathcal{D}$ of size $|\Xi_{\text{train}}^{\mathcal{D}}| = 10^4$. We then specify a two-dimensional submanifold $\mathcal{D}' \equiv [0.75, 1.5]^2 \times \{\mu_{\text{fixed}}\} \subset \mathcal{D}$, where $\mu_{\text{fixed}} = (0.7, 0.8, 0.9, 1.0, 1.1) \in \mathbb{R}^5$, and we perform RB focus calculations with this standard RB model over a 100×100 uniform grid of parameter values, $\Xi_{\text{focus}} \subset \mathcal{D}'$. The RB outputs (evaluated for each $\mu \in \Xi_{\text{train}}^{\mathcal{D}}$ via (2.20)) are shown in Figure 4.1; the RB output error bounds are shown in Figure 4.2 (top).

We then consider the corresponding DRB approach. We generate a DRB model of dimension $M_{\max} = 9$ which satisfies a tolerance $\epsilon_{\text{tol}}^{\text{DRB}} = 10^{-4}$ (with respect to the $N_{\max} = 96$ intermediate RB model) over a uniformly distributed random training set $\Xi_{\text{train}}^{\mathcal{D}'} \subset \mathcal{D}'$ of size $|\Xi_{\text{train}}^{\mathcal{D}'}| = 100$. We then calculate the DRB outputs and DRB output error bounds over Ξ_{focus}; in this case the DRB online computation (including execution of Greedy$^{\text{DRB}}$ and evaluation over Ξ_{focus}) is a factor of 63 faster than the standard RB alternative. Moreover, as shown in Figure 4.2, the maximum output error bounds (with respect to the underlying truth FE approximation) in the standard RB and derived RB approximations are $3.6 \cdot 10^{-5}$ and $1.4 \cdot 10^{-4}$, respectively; hence the DRB yields a significant speedup with only very mild impact on the accuracy of the approximation over $\mathcal{D}'$.

4.2.2 Acoustic Horn

We develop a DRB approximation for the acoustic horn problem introduced in Section 2.2.2 in order to accelerate a focus calculation. We first generate an intermediate RB approximation of dimension $N_{\max} = 109$: we perform Greedy$^{\text{RB}}$

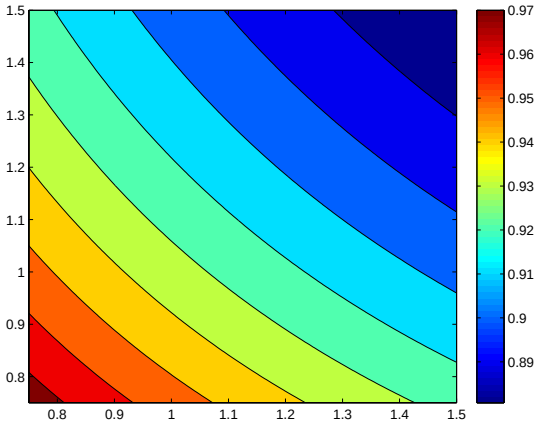

Figure 4.1: The RB output values on $\mathcal{D}'$ for the thermal block; note that the DRB and standard RB outputs are indistinguishable.

for $\mu_1 = (1.4, 2.15, 1.0)$ and $\epsilon_{\text{tol}}^{\text{RB}} = 10^{-4}$ over a uniformly distributed random training set $\Xi_{\text{train}}^{\mathcal{D}} \subset \mathcal{D}$ of size $|\Xi_{\text{train}}^{\mathcal{D}}| = 10^4$. We then specify a one-dimensional slice $\mathcal{D}' \equiv \{\mu_{\text{fixed}}\} \times [0.5, 1.0] \subset \mathcal{D}$, where $\mu_{\text{fixed}} = (1.4, 2.2) \in \mathbb{R}^2$, and we perform RB focus calculations with this standard RB model over a uniform grid of 1000 parameter values, $\Xi_{\text{focus}} \subset \mathcal{D}'$.

We then consider the corresponding DRB approach. We generate a DRB model of dimension $M_{\max} = 11$ which satisfies a tolerance $\epsilon_{\text{tol}}^{\text{DRB}} = 10^{-4}$ (with respect to the $N_{\max} = 109$ intermediate RB model) over a uniformly distributed random training set $\Xi_{\text{train}}^{\mathcal{D}'} \subset \mathcal{D}'$ of size $|\Xi_{\text{train}}^{\mathcal{D}'}| = 1000$. We then calculate the DRB outputs and DRB output error bounds over Ξ_{focus}; in this case the online computation (including execution of Greedy$^{\text{DRB}}$ and evaluation over Ξ_{focus}) is a factor of 10 faster than the standard RB alternative. The focus calculation speedup here is less than for the thermal block because, first, $\mathcal{D}'$ is not so "small" compared to $\mathcal{D}$, and second and more importantly, we perform fewer focus calculations (by a factor of 10). As shown in Figure 4.3, the maximum output error bounds (with respect to the underlying truth FE approximation) in the standard RB and derived RB approximations are $9.8 \cdot 10^{-5}$ and $1.2 \cdot 10^{-4}$, respectively; hence the DRB yields a significant speedup with only very mild impact on the accuracy of the approximation over $\mathcal{D}'$.

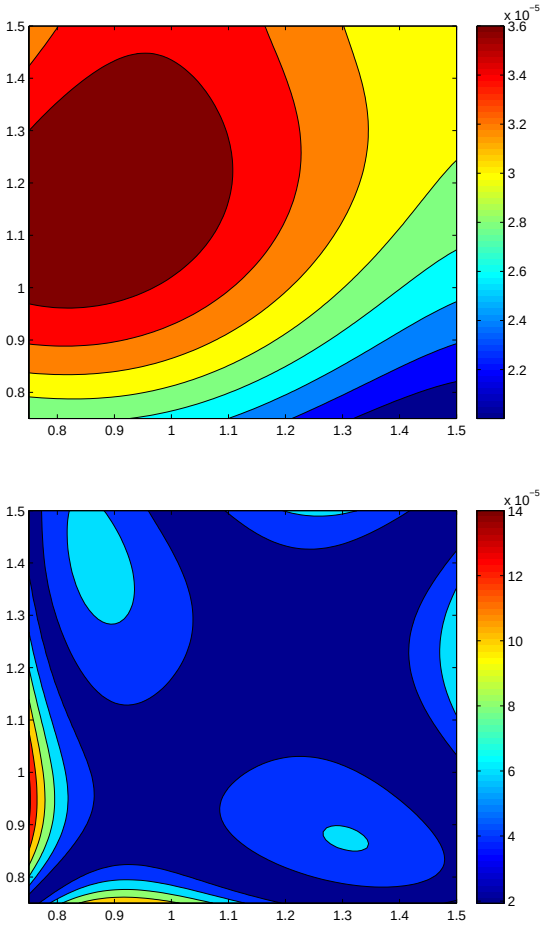

Figure 4.2: Standard RB output error bounds on $\mathcal{D}'$ with respect to the truth discretization (top); and DRB output error bounds on $\mathcal{D}'$ with respect to the truth discretization (bottom).

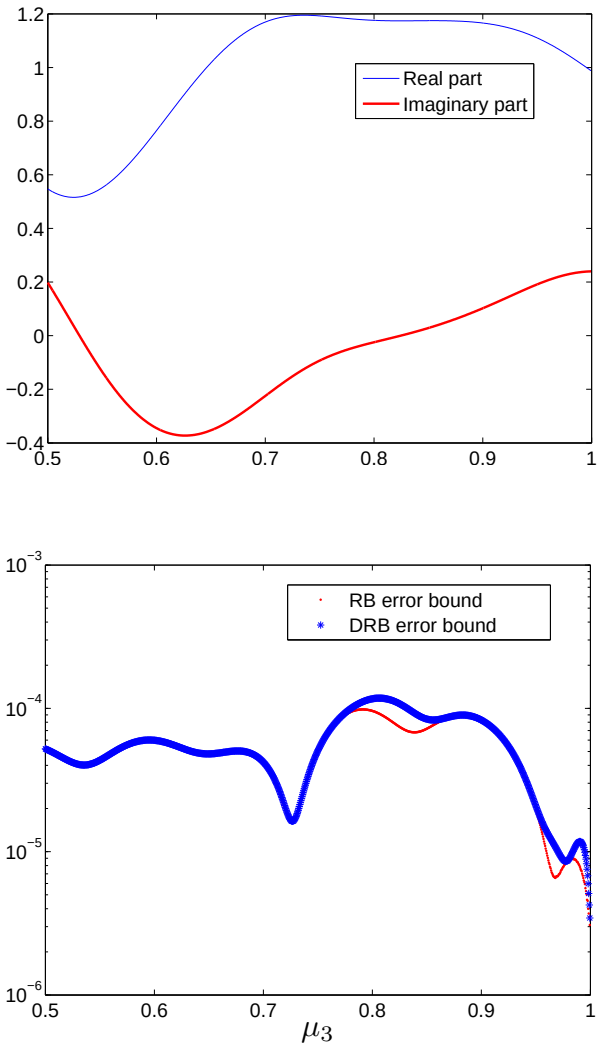

Figure 4.3: The RB output values on $\mathcal{D}'$ for the acoustic horn (top), and the output error bounds on $\mathcal{D}'$ with respect to the truth discretization for the standard RB and DRB approximations (bottom).

5 *hp*-RB Approximation

5.1 Summary of the *hp*-RB Method

The *hp*-RB method introduced in [7] (see also [6, 11]) provides a partition of the parameter domain $\mathcal{D}$ into K parameter subdomains $\mathcal{V}^k \subset \mathcal{D}$, $1 \le k \le K$; for each parameter subdomain $\mathcal{V}^k$, the algorithm generates an associated RB approximation space $X_{N^k}^k \subset X$ of dimension N^k spanned by truth FE snapshots associated with parameter values within $\mathcal{V}^k$. The approach is motivated by order reduction: we may choose the dimension N^k of the "local" space $X_{N^k}^k$ relatively small compared to the dimension N of the "global" space X_N while preserving numerical accuracy. We thus obtain significant speedup of the RB output and RB error bound evaluation. However, the offline (precomputation) cost associated with an *hp*-RB approach is significantly larger than the offline cost associated with the standard RB procedure, and must thus in practice be taken into consideration.

We now review the *hp*-RB method. We first describe the splitting procedure for an arbitrary subdomain $\mathcal{V} \subseteq \mathcal{D}$. Given $\mathcal{V} \subseteq \mathcal{D}$ and a parameter "anchor point" $\mu_1^{\mathcal{V}} \in \mathcal{V}$, we compute the truth FE snapshot $u(\mu_1^{\mathcal{V}})$ and define the one-dimensional "temporary" RB space

$$X_1^{\mathcal{V}} = \text{span}\{u(\mu_1^{\mathcal{V}})\} \tag{5.1}$$

associated with $\mathcal{V}$. We next introduce a finite training set $\Xi_{\text{train}}^{\mathcal{V}} \subset \mathcal{V}$; we then evaluate the RB error bound $\Delta_{N=1}^{\mathcal{V}}$ for the RB approximation associated with the space $X_{N=1}^{\mathcal{V}}$ (essentially (3.9) with an appropriate change of notation) for each parameter value $\mu \in \Xi_{\text{train}}^{\mathcal{V}}$ — essentially one iteration of the Greedy$^{\text{RB}}$ algorithm restricted to $\mathcal{V} \subset \mathcal{D}$ — in order to identify a second parameter value

$$\mu_2^{\mathcal{V}} = \arg \max_{\mu \in \Xi_{\text{train}}^{\mathcal{V}}} \Delta_{N=1}^{\mathcal{V}}(\mu). \tag{5.2}$$

We then split $\mathcal{V}$ into two subdomains $\mathcal{V}_{\text{left}} \subset \mathcal{V}$ and $\mathcal{V}_{\text{right}} \subset \mathcal{V}$ based on (Euclidean, say) distance $\|\cdot\|_2$ to the points $\mu_1^{\mathcal{V}}$ and $\mu_2^{\mathcal{V}}$: any point $\mu \in \mathcal{V}$ belongs to $\mathcal{V}_{\text{left}}$ if and only if $\|\mu - \mu_1^{\mathcal{V}}\|_2 \le \|\mu - \mu_2^{\mathcal{V}}\|_2$; otherwise, $\mu \in \mathcal{V}$ belongs to $\mathcal{V}_{\text{right}}$. Finally, we define $\mu_1^{\mathcal{V}}$ as the anchor point for $\mathcal{V}_{\text{left}}$ and we define $\mu_2^{\mathcal{V}}$ as the anchor point for $\mathcal{V}_{\text{right}}$.

We may now describe the *hp*-RB method. The first step is *h*-refinement: We apply the splitting scheme discussed above for $\mathcal{V} = \mathcal{D}$, and then recursively for $\mathcal{V} = \mathcal{V}_{\text{left}}$ and $\mathcal{V} = \mathcal{V}_{\text{right}}$ (sketched in Figure 5.1 for two levels of splitting). We terminate the splitting of a subdomain $\mathcal{V}$ if $\max_{\mu \in \Xi_{\text{train}}^{\mathcal{V}}} \Delta_{N=1}^{\mathcal{V}}(\mu) \le \epsilon_{\text{tol}}^h$, where ϵ_{tol}^h is a specified tolerance for the *h*-refinement step. The result of this hierarchical procedure is $K = K(\epsilon_{\text{tol}}^h)$ parameter subdomains $\mathcal{V}^k \subset \mathcal{D}$, $1 \le k \le K$.

The next step is *p*-refinement: Greedy construction of the approximation spaces $X_{N^k}^k$, $1 \le k \le K$. We here choose N^k, $1 \le k \le K$, such that a specified tolerance $\epsilon_{\text{tol}}^p \le \epsilon_{\text{tol}}^h$ is satisfied over training sets $\Xi_{\text{train}}^{\mathcal{V}^k} \subset \mathcal{V}^k$, $1 \le k \le K$. Note

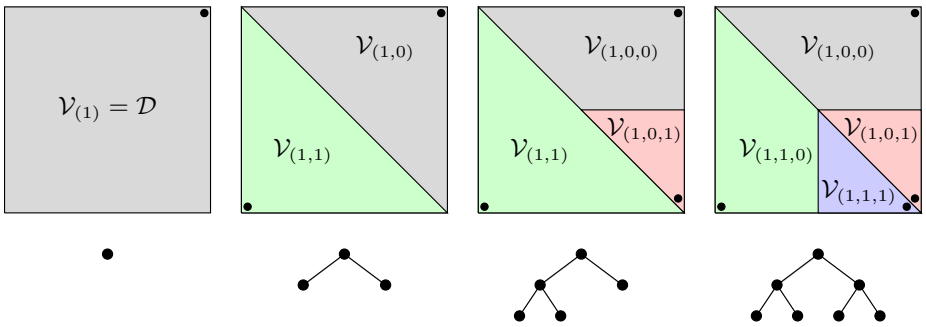

Figure 5.1: h-refinement partition procedure.

that this step is essentially execution of the Greedy$^{\text{RB}}$ algorithm for $\epsilon_{\text{tol}}^{\text{RB}} = \epsilon_{\text{tol}}^{p}$ restricted to each subdomain $\mathcal{V}^k \subset \mathcal{D}$, $1 \le k \le K$.

In practice, we also apply if necessary an additional splitting step (see [6]) after the p-refinement. Essentially, this step performs additional h-refinement of a subdomain if $\epsilon_{\text{tol}}^{p}$ is not satisfied for specified $N_{\max}^{hp}$ basis functions. The additional splitting proceeds recursively with h-refinement and p-refinement steps until $\epsilon_{\text{tol}}^{p}$ is satisfied for $N_{\max}^{hp}$ basis functions, thus providing for direct control of the tolerance $\epsilon_{\text{tol}}^{p}$ *and* the RB space dimension.

Thanks to the hierarchical construction of the partition, we may organize the subdomains (and associated approximation spaces) as the leaf nodes in a binary tree with Boolean flags, as illustrated in Figure 5.1. This tree-structure partiton is important in the hp-RB online stage: the cost to determine which subdomain $\mathcal{V}^{k^*}$ contains any given $\mu \in \mathcal{D}$ is $\mathcal{O}(\log(K))$ for K subdomains [7].

The hp-RB approximation reads as follows: first, given any $\mu \in \mathcal{D}$, determine $k^* = k^*(\mu) \in [1, K]$ and hence $\mathcal{V}^{k^*}$ and $X_{N^{k^*}}^{k^*}$ through a binary search; given $1 \le N \le N_{\max}^{hp}$, we write $\hat{N} = \min\{N, N^{k^*}\}$ and $X_N^{hp} = X_{\hat{N}}^{k^*}$. Then, determine $u_N^K(\mu) \in X_N^{hp}$ such that

$$a(u_N^K(\mu), v; \mu) = f(v; \mu), \quad \forall v \in X_N^{hp}; \tag{5.3}$$

finally evaluate the hp-RB output approximation

$$s_N^K(\mu) = \ell(u_N^K(\mu)). \tag{5.4}$$

We define the hp-RB error bound as

$$\Delta_N^K(\mu) = \frac{\|\mathcal{R}_N^K(\mu)\|_X}{\alpha_{\text{LB}}(\mu)}, \tag{5.5}$$

where $\mathcal{R}_N^K(\mu) \in X$ denotes the Riesz representation of the residual

$$r_N^K(\cdot; \mu) = f(\cdot; \mu) - a(u_N^K(\mu), \cdot; \mu) \in X'. \tag{5.6}$$

We may readily show that $\|u(\mu) - u_N^K(\mu)\|_X \le \Delta_N^K(\mu)$ by arguments analogous to (3.10)–(3.12).

5.2 DRB Modification

We now discuss the application of the two-step RB approach within the *hp*-RB context. We introduce a "global" intermediate RB approximation space $X_{N_{\max}}$ of dimension $N_{\max}$ constructed by Greedy$^{\text{RB}}$ (Algorithm 1) for a specified initial parameter value $\mu_1 \in \mathcal{D}$ and a specified error bound tolerance $\epsilon_{\text{tol}}^{\text{RB}}$ (to be satisfied over the training set $\Xi_{\text{train}}^{\mathcal{D}} \subset \mathcal{D}$). The necessary modifications to the *hp*-RB method discussed in the previous subsection are then as follows. First, during the *h*-refinement step we replace the truth snapshot $u(\mu_1^{\mathcal{V}})$ by an RB snapshot $u_{N_{\max}}(\mu_1^{\mathcal{V}}) \approx u(\mu_1^{\mathcal{V}})$; we thus replace the RB space $X_1^{\mathcal{V}}$ in (5.1) by the DRB space

$$X_{N_{\max},1}^{\mathcal{V}} = \text{span}\{u_{N_{\max}}(\mu_1^{\mathcal{V}})\}. \tag{5.7}$$

We further replace the RB error bound $\Delta_{N=1}^{\mathcal{V}}$ in (5.2) by a DRB error bound $\tilde{\Delta}_{N_{\max},M=1}^{\mathcal{V}}$ (essentially (3.17) with an appropriate change of notation). We then invoke this DRB error bound (with respect to the underlying RB approximation) to determine a second parameter value

$$\mu_2^{\mathcal{V}} = \arg\max_{\mu \in \Xi^{\mathcal{V}}} \tilde{\Delta}_{N_{\max},M=1}^{\mathcal{V}}(\mu). \tag{5.8}$$

As before, $\mu_1^{\mathcal{V}}$ and $\mu_2^{\mathcal{V}}$ determine the splitting of $\mathcal{V}$ into $\mathcal{V}_{\text{left}}$ and $\mathcal{V}_{\text{right}}$. Note that we terminate the splitting of a subdomain $\mathcal{V}$ if $\max_{\mu \in \Xi_{\text{train}}^{\mathcal{V}}} \tilde{\Delta}_{N_{\max},M=1}^{\mathcal{V}}(\mu) \le \epsilon_{\text{tol}}^{h}$; typically $\epsilon_{\text{tol}}^{h}$ is chosen much greater than $\epsilon_{\text{tol}}^{\text{RB}}$. As before, we apply the splitting procedure recursively until convergence; the result is $K = K(\epsilon_{\text{tol}}^{h})$ subdomains $\mathcal{V}^k \subset \mathcal{D}$, $1 \le k \le K$.

Next, in the *p*-refinement step, we associate to each $\mathcal{V}^k$ a DRB approximation space $X_{N_{\max},M^k}$, $1 \le k \le K$; the *p*-refinement step is thus essentially execution of Greedy$^{\text{DRB}}$ for $\epsilon_{\text{tol}}^{\text{RB}} = \epsilon_{\text{tol}}^{p}$ restricted to each $\mathcal{V}^k$, $1 \le k \le K$. We typically choose $\epsilon_{\text{tol}}^{p}$ such that $\epsilon_{\text{tol}}^{\text{RB}} \le \epsilon_{\text{tol}}^{p} < \epsilon_{\text{tol}}^{h}$. As before, we apply in practice an additional splitting step which provides simultaneous control over the tolerance $\epsilon_{\text{tol}}^{p}$ *and* the maximum DRB space dimension $M_{\max}^{hp}$.

With the modificatins above, the *hp*-DRB approximation reads as follows: first, given any $\mu \in \mathcal{D}$, determine $k^* = k^*(\mu)$ and hence $\mathcal{V}^{k^*}$ and $X_{N_{\max},M^{k^*}}^{k^*}$ through a binary search; given $1 \le M \le M_{\max}^{hp}$, we write $\hat{M} = \min\{M, M^{k^*}\}$ and $X_{N_{\max},M}^{hp} = X_{N_{\max},\hat{M}}^{k*}$. Then, determine $u_{N_{\max},M}^{K}(\mu) \in X_{N_{\max},M}^{hp}$ such that

$$a(u_{N_{\max},M}^{K}(\mu), v; \mu) = f(v; \mu), \quad \forall v \in X_{N_{\max},M}^{hp}; \tag{5.9}$$

finally evaluate the *hp*-DRB output approximation

$$s_{N_{\max},M}^{K}(\mu) = \ell(u_{N_{\max},M}^{K}(\mu)). \tag{5.10}$$

We define the *hp*-DRB error bound as

$$\Delta_{N_{\max},M}^{K}(\mu) = \frac{\|\mathcal{R}_{N_{\max},M}^{K}(\mu)\|_X}{\alpha_{\text{LB}}(\mu)}, \tag{5.11}$$

where $\mathcal{R}^K_{N_{\max},M}(\mu) \in X$ denotes the Riesz representation of the residual

$$r^K_{N_{\max},M}(\cdot;\mu) = f(\cdot;\mu) - a(u^K_{N_{\max},M}(\mu),\cdot;\mu) \in X'. \tag{5.12}$$

We may readily show that $\|u(\mu) - u^K_{N_{\max},M}(\mu)\|_X \le \Delta^K_{N_{\max},M}(\mu)$ by arguments analogous to (3.10)–(3.12). We recall from our discussion in Section 3.4.2 that we may evaluate $\Delta^K_{N_{\max},M}(\mu)$ inexpensively at cost independent of $\mathcal{N}$ *and* N.

We emphasize that with these modifications we access entities of truth complexity $\mathcal{N}$ only for the construction of the intermediate RB model (of complexity $N \ll \mathcal{N}$) upon which the *hp*-DRB approximation is constructed. We discuss the offline-online decoupling of the *hp*-DRB method in the next subsection.

5.3 Offline–Online Decomposition

The *hp*-DRB *offline* stage comprises intermediate RB model construction and then *hp*-DRB partition and approximation space construction based on this underlying RB model.

1. RB model construction. We construct an intermediate RB model over $\mathcal{D}$: we perform Greedy$^{\text{RB}}$ (Algorithm 1) for specified $\mu_1 \in \mathcal{D}$ and $\epsilon^{\text{RB}}_{\text{tol}}$. The cost is $\mathcal{N}$-dependent.

2. *hp*-DRB partition and approximation space construction. We construct an *hp*-DRB model based on the intermediate RB model in step 1 as discussed in the previous two subsections. This step includes, for each DRB approximation space, construction of the parameter-independent entities required for DRB output and DRB error bound evaluation. The cost is $\mathcal{N}$-independent.

The offline stage may be expensive; however with the DRB modification in step 2 above we significantly reduce the offline computational cost compared to a standard *hp*-RB approach: the $N_{\text{total}} = \sum_{k=1}^K N^k$ truth FE snapshots of $\mathcal{N}$-dependent complexity required by the standard *hp*-RB offline stage are replaced by $M_{\text{total}} = \sum_{k=1}^K M^k$ RB snapshots of $N_{\max}$-dependent complexity.[6]

In the online stage, given any new parameter value $\mu \in \mathcal{D}$, we first determine which subdomain $\mathcal{V}^{k^*} \subset \mathcal{D}$ contains μ through a binary search at cost $\mathcal{O}(\log K)$. Then, for given $1 \le M \le M^{hp}_{\max}$, we compute the DRB solution, DRB output, and DRB error bound at cost $\mathcal{O}(M^3 + M^2Q^2)$. We note that the online cost is independent of the truth complexity $\mathcal{N}$ *and* the complexity N associated with the underlying intermediate RB model. We emphasize that in the online stage, we invoke the DRB error bound with respect to the FE truth approximation.

We finally note that the offline–online decomposition associated with the *hp*-DRB approximation is rather different from the offline–online decomposition associated with focus calculations: the DRB "technology" is invoked in the offline (and not online) stage.

[6] Note that we expect here that $M^k \approx N^k$ as long as M^k is significantly smaller than $N_{\max}$, $1 \le k \le K$. Also note that for simplicity in this argument we assume that K is the same for the *hp*-RB and *hp*-DRB approaches.

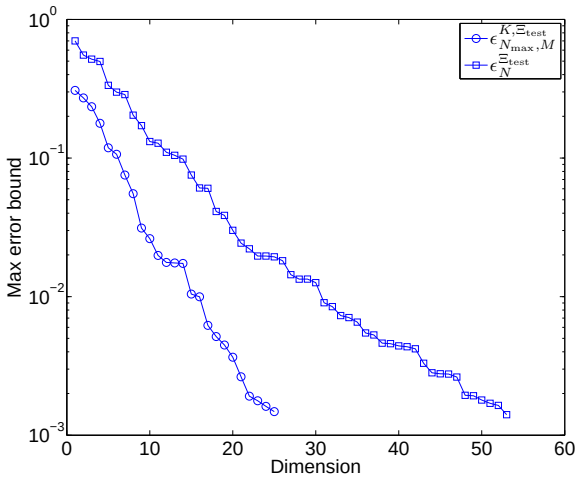

Figure 5.2: Maximum RB (squares) and *hp*-DRB (circles) error bounds over random test parameter values as a function of approximation space dimension.

5.4 Numerical Results

5.4.1 Thermal Block

We now apply the *hp*-DRB method to the thermal block problem introduced in Section 2.2.1. For the underlying intermediate RB space $X_{N_{\max}}$ we use the same space as for the thermal block focus calculation example: $N_{\max} = 96$. We then pursue the *hp*-DRB procedure discussed above for $\epsilon^h_{\text{tol}} = 0.3$, $\epsilon^p_{\text{tol}} = 10^{-3}$, and $M^{hp}_{\max} = 25$; the initial parameter value for the partition procedure is $\mu^{\mathcal{D}}_1 = (0.5, 0.5, 0.5, 0.5, 0.5, 0.5, 0.5)$. The *hp*-DRB offline computation results in a partition of $\mathcal{D}$ into $K = 7565$ subdomains, each of which has an associated DRB approximation space of dimension at most $M^{hp}_{\max} = 25$.

We now introduce a uniformly distributed random test set $\Xi_{\text{test}} \subset \mathcal{D}$ of size $|\Xi_{\text{test}}| = 1000$. We then define, for $1 \le N \le N_{\max}$, the maximum error bound associated with the RB approximation,

$$\epsilon^{\Xi_{\text{test}}}_N = \max_{\mu \in \Xi_{\text{test}}} \Delta_N(\mu); \tag{5.13}$$

we also define, for $1 \le M \le M^{hp}_{\max}$, the maximum error bound associated with the *hp*-DRB approximation,

$$\epsilon^{K,\Xi_{\text{test}}}_{N_{\max},M} = \max_{\mu \in \Xi_{\text{test}}} \Delta^K_{N_{\max},M}(\mu). \tag{5.14}$$

In Figure 5.2 we compare $\epsilon^{\Xi_{\text{test}}}_N$ and $\epsilon^{K,\Xi_{\text{test}}}_{N_{\max},M}$ as functions of the approximation space dimensions N and M, respectively: clearly the *hp*-DRB approximation provides significant dimension reduction. For example, $N = 30$ and $M = 15$

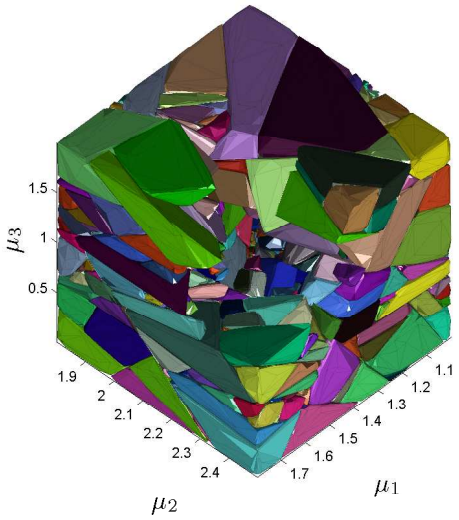

Figure 5.3: The parameter domain partition associated with the *hp*-DRB approximation for the acoustic horn problem; note that one octant of the parameter domain is hidden.

basis functions are required for an error bound of approximately 10^{-2} for the RB and *hp*-DRB approximation, respectively. The *hp*-DRB thus provide in this case online computational savings by a factor of 8 (provided the dense system matrix LU-factorization dominates online cost).

The main point of this example is not the dimension reduction provided by the *hp*-DRB procedure *per se*: we would have obtained similar dimension reduction were we to use a standard *hp*-RB procedure. Our emphasis here is on the offline stage, which requires 232608 snapshots: this task is feasible in the *hp*-DRB case in which each snapshot is an RB calculation ($N_{\max} = 96$ degrees of freedom), but would clearly be prohibitive in the standard *hp*-RB case in which each snapshot is a *truth* calculation ($\mathcal{N} = 9261$ degrees of freedom).

5.4.2 Acoustic Horn

We now apply the *hp*-DRB method to the acoustic horn problem introduced in Section 2.2.2. For the underlying intermediate RB space $X_{N_{\max}}$ we use the same space as for the acoustic horn focus calculation example: $N_{\max} = 109$. We then pursue the *hp*-DRB procedure discussed above for $\epsilon_{\text{tol}}^h = 10$, $\epsilon_{\text{tol}}^p = 10^{-4}$, and $M_{\max}^{hp} = 30$; the initial parameter value for the partition procedure is $\mu_1^{\mathcal{D}} = (1.4, 2.15, 1.0)$. The *hp*-DRB offline computation results in a partition of $\mathcal{D}$ into $K = 997$ subdomains as shown in Figure 5.3, each of which has an associated DRB approximation space of dimension at most $M_{\max}^{hp} = 30$.

We now introduce a uniformly distributed random test set $\Xi_{\text{test}} \subset \mathcal{D}$ of size $|\Xi_{\text{test}}| = 1000$ and show in Figure 5.4 $\epsilon_N^{\Xi_{\text{test}}}$ and $\epsilon_{N_{\max},M}^{K,\Xi_{\text{test}}}$ as functions of the

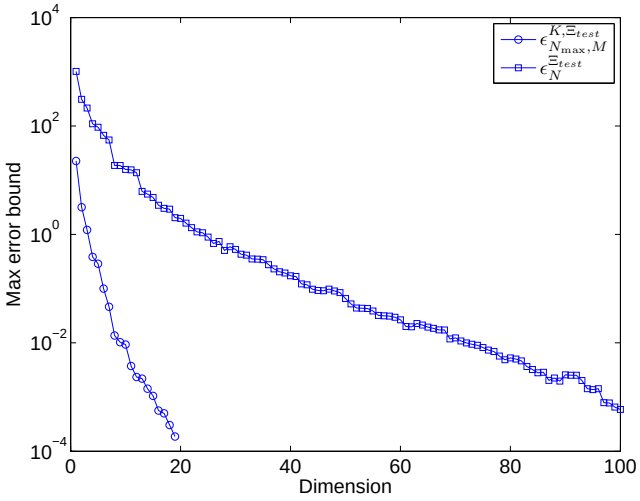

Figure 5.4: Maximum RB (squares) and *hp*-DRB (circles) error bounds over random test parameter values as a function of approximation space dimension.

approximation space dimensions N and M, respectively: clearly the *hp*-DRB approximation provides significant dimension reduction. As for the thermal block example, our main point here is that the DRB strategy enables a feasible *hp*-DRB offline computation, compared to a prohibitive or infeasible *hp*-RB offline computation.

6 Conclusions and Future Work

We have demonstrated that the new DRB method may provide significant online speedup in the context of focus calculations, for example for visualization or optimization of RB outputs and RB error bounds over a subdomain or submanifold of the original parameter domain. Further, we have demonstrated that the DRB method may provide significant offline speedup for *hp*-RB computations, or indeed enable *hp*-RB computations for problems for which the cost of the standard *hp*-RB offline stage is prohibitive.

There are several opportunities for extensions. First, the DRB method readily extends to linear parabolic (coercive or non-coercive) problems; we refer to [9, 12] and [6] for (standard) RB and *hp*-RB treatment of this class of problems, respectively. We may also straightforwardly apply the DRB approach to quadratically nonlinear problems; see [6] for *hp*-RB treatment of the unsteady incompressible Navier-Stokes equations. Second, we believe that the DRB method will further increase the efficacy of the RB method in applications on "lightweight" hardware [15] where it is crucial to minimize the cost of a reduced order model both in terms of computation time and memory footprint.

In future work we plan to investigate applications of DRB technology in a range of new areas such as *in situ* parameter estimation, uncertainty quantification and design/optimization.

Acknowledgements

This work has been supported by AFOSR Grant number FA9550-07-1-0425, OSD/AFOSR Grant number FA9550-09-1-0613, and the Norwegian University of Science and Technology.

References

[1] B. O. Almroth, P. Stern, and F. A. Brogan. Automatic choice of global shape functions in structural analysis. *AIAA Journal*, 16:525–528, 1978.

[2] M. Barrault, N. C. Nguyen, Y. Maday, and A. T. Patera. An "empirical interpolation" method: Application to efficient reduced-basis discretization of partial differential equations. *C. R. Acad. Sci. Paris, Série I.*, 339:667–672, 2004.

[3] S. Boyaval. Reduced-basis approach for homogenization beyond the periodic setting. *Multiscale Model. Simul.*, 7(1):466–494, 2008.

[4] S. Boyaval, C. Le Bris, Y. Maday, N. C. Nguyen, and A. T Patera. A reduced basis approach for variational problems with stochastic parameters: Application to heat conduction with variable robin coefficient. *Computer Methods in Applied Mechanics and Engineering*, 198(41-44):3187 – 3206, 2009.

[5] C. Canuto, T. Tonn, and K. Urban. A posteriori error analysis of the reduced basis method for nonaffine parametrized nonlinear PDEs. *SIAM Journal on Numerical Analysis*, 47(3):2001–2022, 2009.

[6] J. L. Eftang, D. J. Knezevic, and A. T. Patera. An *hp* Certified Reduced Basis Method for Parametrized Parabolic Partial Differential Equations. Accepted in Mathematical and Computer Modelling of Dynamical Systems, 2011.

[7] J. L. Eftang, A. T. Patera, and E. M. Rønquist. An "*hp*" certified reduced basis method for parametrized elliptic partial differential equations. *SIAM Journal on Scientific Computing*, 32(6):3170–3200, 2010.

[8] G. H. Golub and C. F. Van Loan. *Matrix computations*. Johns Hopkins Studies in the Mathematical Sciences. Johns Hopkins University Press, Baltimore, MD, third edition, 1996.

[9] M. A. Grepl and A. T. Patera. A posteriori error bounds for reduced-basis approximations of parametrized parabolic partial differential equations. *M2AN*, 39(1):157–181, 2005.

[10] M.A. Grepl, Y. Maday, N.C. Nguyen, and A.T. Patera. Efficient reduced basis treatment of nonaffine and nonlinear partial differential equations. *ESAIM: M2AN*, 41(3):575–605, 2007.

[11] B. Haasdonk, M. Dihlmann, and M. Ohlberger. A Training Set and Multiple Bases Generation Approach for Parametrized Model Reduction Based on Adaptive Grids in Parameter Space. Technical Report 28, SRC SimTech, 2010.

[12] B. Haasdonk and M. Ohlberger. Reduced basis method for finite volume approximations of parametrized linear evolution equations. *ESAIM: M2AN*, 42(2):277–302, 2008.

[13] B. Haasdonk and M Ohlberger. Efficient reduced models and a posteriori error estimation for parametrized dynamical systems by offline/online decomposition. *Mathematical and Computer Modelling of Dynamical Systems*, 2011. `http://dx.doi.org/10.1080/13873954.2010.514703`.

[14] D. B. P. Huynh, D. J. Knezevic, and A. T. Patera. Certified reduced basis model characterization: a frequentistic uncertainty framework. Computer Methods in Applied Mechanics and Engineering (submitted January 2011). `http://augustine.mit.edu/methodology/papers/atp_CMAME_preprint_Jan2011.pdf`.

[15] D. B. P. Huynh, D. J. Knezevic, J. W. Peterson, and A. T. Patera. High-fidelity real-time simulation on deployed platforms. *Computers & Fluids*, In Press, Corrected Proof:–, 2010. DOI: 10.1016/j.compfluid.2010.07.007.

[16] D. B. P. Huynh, D.J. Knezevic, Y. Chen, J.S. Hesthaven, and A.T. Patera. A natural-norm successive constraint method for inf-sup lower bounds. *Computer Methods in Applied Mechanics and Engineering*, 199(29-32):1963 – 1975, 2010.

[17] D. B. P. Huynh, G. Rozza, S. Sen, and A.T. Patera. A successive constraint linear optimization method for lower bounds of parametric coercivity and inf-sup stability constants. *Comptes Rendus Mathematique*, 345(8):473 – 478, 2007.

[18] M. Kamon, F. Wang, and J. White. Generating nearly optimally compact models from Krylov-subspace based reduced-order models. *Circuits and Systems II: Analog and Digital Signal Processing, IEEE Transactions on*, 47(4):239 –248, apr. 2000.

[19] B. S. Kirk, J. W. Peterson, R. H. Stogner, and G. F. Carey. `libMesh`: A C++ Library for Parallel Adaptive Mesh Refinement/Coarsening Simulations. *Engineering with Computers*, 22(3–4):237–254, 2006.

[20] D. J. Knezevic and A. T. Patera. A certified reduced basis method for the fokker–planck equation of dilute polymeric fluids: Fene dumbbells in extensional flow. *SIAM Journal on Scientific Computing*, 32(2):793–817, 2010.

[21] D. J. Knezevic and J. W. Peterson. A high-performance parallel implementation of the certified reduced basis method. *Computer Methods in Applied Mechanics and Engineering (submitted)*, 2010.

[22] B. Moore. Principal component analysis in linear systems: Controllability, observability, and model reduction. *Automatic Control, IEEE Transactions on*, 26(1):17 – 32, feb. 1981.

[23] N. C. Nguyen, G. Rozza, D. B. P. Huynh, and A. T. Patera. *Reduced Basis Approximation and a Posteriori Error Estimation for Parametrized Parabolic PDEs: Application to Real-Time Bayesian Parameter Estimation*, pages 151–177. John Wiley & Sons, Ltd, 2010.

[24] A. K. Noor and J. M. Peters. Reduced basis technique for nonlinear analysis of structures. *AIAA Journal*, 18:455–462, 1980.

[25] T. A. Porsching. Estimation of the error in the reduced basis method solution of nonlinear equations. *Math. Comp.*, 45:487–496, 1985.

[26] G. Rozza, D. B. P. Huynh, and A. T. Patera. Reduced Basis Approximation and *a posteriori* Error Estimation for Affinely Parametrized Elliptic Coercive Partial Differential Equations. *Archives of Computational Methods in Engineering*, 15(3):229–275, 2008.

[27] R. Udawalpola and M. Berggren. Optimization of an acoustic horn with respect to efficiency and directivity. *International Journal for Numerical Methods in Engineering*, 73:1571–1606, 2008.

[28] K. Veroy, C. Prud'homme, D. V. Rovas, and A. T. Patera. A posteriori error bounds for reduced-basis approximation of parametrized noncoercive and nonlinear elliptic partial differential equations. In *Proceedings of the 16th AIAA Computational Fluid Dynamics Conference*, pages AIAA Paper 2003–3847, 2003.

[29] K. Willcox and A. Megretski. Fourier series for accurate, stable, reduced-order models in large-scale linear applications. *SIAM J. Sci. Comput.*, 26(3):944–962 (electronic), 2005.